
Deep Submodular Peripteral Networks

Gantavya Bhatt ^{*}
 University of Washington
 Seattle, WA 98195
 gbhatt2@uw.edu

Arnav M. Das ^{*}
 University of Washington
 Seattle, WA 98195
 arnavmd2@uw.edu

Jeffery A. Bilmes
 University of Washington
 Seattle, WA 98195
 bilmes@uw.edu

Abstract

Submodular functions, crucial for various applications, often lack practical learning methods for their acquisition. Seemingly unrelated, learning a scaling from oracles offering graded pairwise preferences (GPC) is underexplored, despite a rich history in psychometrics. In this paper, we introduce deep submodular peripteral networks (DSPNs), a novel parametric family of submodular functions, and methods for their training using a contrastive-learning inspired GPC-ready strategy to connect and then tackle both of the above challenges. We introduce newly devised GPC-style “peripteral” loss which leverages numerically graded relationships between pairs of objects (sets in our case). Unlike traditional contrastive learning, our method utilizes graded comparisons, extracting more nuanced information than just binary-outcome comparisons, and contrasts sets of any size (not just two). We also define a novel suite of automatic sampling strategies for training, including active-learning inspired submodular feedback. We demonstrate DSPNs’ efficacy in learning submodularity from a costly target submodular function showing superiority in downstream tasks such as experimental design and streaming applications.

1 Introduction and Background

This paper jointly addresses two seemingly disparate problems presently open in the machine learning community.

The first is that of identifying a useful practical scalable submodular function that can be used for real-world data science tasks. Submodular functions have received considerable attention in the field of machine learning, leading to the creation of algorithms that offer near-optimal solutions for various applications. These applications include detecting disease outbreaks Leskovec et al. [2007], modeling fine structure in computer vision Jegelka and Bilmes [2011], summarizing images Tschiatschek et al. [2014], Mitrovic et al. [2018], Feldman et al. [2018], Harshaw et al. [2022], active learning Guillory and Bilmes [2011], Golovin and Krause [2010], Esfandiari et al. [2021], compressed sensing, structured convex norms, and sparsity Bach [2010], Elenberg et al. [2018], fairness Celis et al. [2016], Kazemi et al. [2021], efficient model training Lin and Bilmes [2009, 2010], Mirzasoleiman et al. [2016, 2020] recommendation systems Mitrovic et al. [2019], causal structure Zhou and Spanos [2016], Sussex et al. [2021], and brain parcellating Salehi et al. [2017] (see also the reviews Tohidi et al. [2020], Bilmes [2022]). Despite these myriad applications, most research on submodularity has been on the algorithmic and theoretical side which assumes the submodular function needing to be

^{*}Equal Contribution

optimized is already at hand. While there has been work showing the theoretical challenges associated with learning submodularity Balcan et al. [2011, 2016], Balcan and Harvey [2018], there is relatively little work on practical methods to produce a useful submodular function in the first place (exceptions include Lin and Bilmes [2012], Sipos et al. [2011], Tschiatschek et al. [2018]). Often, because it works well, one uses the non-parametric submodular facility location (FL) function, i.e., for $A \subseteq V$ with $|V| = n$, $f(A) = \sum_{i=1}^n \max_{a \in A} s_{a,i}$ where $s_{a,i} \geq 0$ is a similarity between items a and i . On the other hand, the FL function’s computational and memory costs grow quadratically with dataset size n and so FL is infeasible for large data or online streaming applications. There is a need for practical strategies to obtain useful, scalable, general-purpose, and widely applicable submodular functions.

The second problem addressed in this paper is the following: how best, in a modern machine-learning context, can one learn a scaling from oracles that, for a given query, each provide numerically graded pairwise comparisons between two choices? That is, given two choices, A and B , an oracle provides a score $Score(A, B) \in \mathbb{R}$ which is positive if A is preferred to B , negative if B is preferred to A , zero if indifferent, and where the absolute value provides the degree of preference A or B has over the other. The oracle could be an individual human annotator, or could be a combinatorially expensive desired target function — in either case we assume that while it is infeasible to optimize over the oracle, it is feasible to query.

A special case of such preference elicitation from human oracles have been studied going back many decades. For example, the psychometric “Law of comparative judgment” Thurstone [1927] focuses on establishing numeric interval scales based on knowing preferences between pairs of choices (e.g., A vs B). The Bradley-Terry Bradley and Terry [1952] model (generalized to ranking elicitations in the Luce-Shephard model Luce [1959], Shepard [1957]) also involves preferences among elements of pairs. These preferences, however, are not graded and rather are either only binary ($A \prec B$ or $B \prec A$), ternary (allowing also for indifference), or quaternary (allowing also for incomparability). Thus, each oracle query provides minimal information about a pair. Therefore, multiple preference ratings are often aggregated where a collection of (presumed random i.i.d.) oracles vote on the preference between items of the same pair. This produces a histogram of preference ratings C_{ij} (a count of how many times i is preferred to j Silverstein and Farrell [2001]) and this can be used in modern reinforcement learning with human feedback (RLHF) systems Wirth et al. [2017], Christiano et al. [2023], Ouyang et al. [2022], Zhan et al. [2023], Wang et al. [2023] for reward learning (i.e., inverse reinforcement learning Arora and Doshi [2021], Adams et al. [2022]). Overall, the above modeling strategies are known in the field of psychometric theory Guilford [1954] as “paired comparisons” where it is said that “paired comparison methods generally give much more reliable results” Nunnally and Bernstein [1994] for models of human preference expression and elicitation.

There are other models of preference elicitation besides paired comparisons, however. Our aforementioned desire is for “graded pairwise comparisons” (GPC) which also have been studied for quite some time Scheffe [1952], Bechtel [1967, 1971]. Quite recently, it was found that “GPCs are expected to reduce faking compared with Likert-type scales and to produce more reliable, less ipsative [the extent to which results are influenced by the specific method of measurement] trait scores than traditional-binary forced-choice formats” Lingel et al. [2022] such as paired comparisons. An intuitive reason for this is that, once we get to the point that an oracle is asked only if $A \prec B$ or $B \prec A$, this does not elicit as much information out of the oracle as would asking for $Score(A, B)$ even though the incremental oracle effort for the latter is often negligible. As far as we know, despite GPC’s potential information extraction efficiency advantages, GPC has not been addressed in the modern machine learning community. Also, while histograms $C_{i,j}$ are appropriate for maximum likelihood estimation (MLE) of non-linear logistic and softmax style regression Christiano et al. [2023], Ouyang et al. [2022], Zhu et al. [2023], Zhan et al. [2023], MLE with a Bradley-Terry style model is suboptimal to learn scoring from graded preferences $Score(A, B) \in \mathbb{R}$ which can be an arbitrary signed real number.

In the present paper we simultaneously address both of the above concerns via the introduction and training of **deep submodular peripetal networks** (DSPNs). In a nutshell, DSPNs are an expressive theoretically interesting parametric family of submodular functions that can be successfully learnt using a new GPC-style loss that we introduce below.

We are inspired by contrastive learning Balestrieri et al. [2023], which has pushed the boundaries of deep learning by leveraging the massive information in unlabeled data. Unlike standard supervised learning which teaches models to associate samples to human-supplied labels, contrastive learning

encourages models to capture relationships between pairs, groups, or sections of unlabeled samples. It does this by “contrasting” positive pairs (i.e., similar data points) against negative pairs (dissimilar data points). Mathematically, this approach uses loss functions that encourage the model to learn embeddings where positive pairs become “close” (according to some distance measure), while negative pairs become “far.” A common setting is the contrastive loss, such as the triplet loss or the Siamese network loss. For instance, in the triplet loss framework, the model is trained on triplets of data points consisting of an anchor x , a positive example x^+ (similar to the anchor), and a negative example x^- (dissimilar from the anchor). Optimizing a model with such a loss function encourages a representation that respects these positive/negative pairwise preferences.

On the other hand, such contrastive approaches are analogous to binary-only pairwise comparison elicitations. That is, existing contrastive losses neither utilize information regarding how positive the pair x, x^+ is nor how negative the pair x, x^- is. A more nuanced graded comparison, if available, would be an improvement. In fact, the benefit of graded comparisons is analogous to the benefits of using soft over hard labels in supervised training (say from model distillation) which has benefits in uncertainty representation, regularization, noise mitigation, adjustable smoothness via softmax temperature, and more efficient knowledge transfer. Another limitation of previous contrastive learning is that it operates only with positive or negative groups of size two (pairs) rather than larger groups. While it is often the case that the anchor x is contrasted with many negative examples, it is always done so pairwise, considering each x^- with x together in a sum of pairwise terms. Also, while Tian et al. [2020] is the only work we are aware of that considers more than two positive examples at a time, each of these positive samples is again considered only paired up with a negative sample, leading to $\binom{k}{2}$ pairings with k positive examples. Sums of pairwise terms do not allow for the consideration of higher order relationships, e.g., a given pair might be measured differently in the context of a third sample. In addition to addressing the two aforementioned problems, DSPNs and our GPC-style loss addresses this issue as well, although our learning goal in this paper is learning submodularity not in representation learning (the latter of which we leave to future work).

An outline of our paper follows. In §2 we define the class of DSPN functions, motivating the name “peripetal”, and offering theoretical comparisons with the class of deep sets Zaheer et al. [2017]. Next, §3 describes a new GPC-style “peripetal” loss that is appropriate to train a DSPN but can be used in any GPC-based preference elicitation learning task. For DSPN learning, this happens by producing a list of pairs of subsets E, M that can be used to transfer information from the oracle target to the DSPN being learnt. §4 describes several E, M pair sampling strategy including an active-learning inspired submodular feedback approach. §5 empirically evaluates DSPN learning based on how effectively information is transferred from the target oracle and performance on downstream tasks such as experimental design. We find that the peripetal loss outperforms other losses for training DSPNs, and show that the DSPN architecture is more effective at learning from the target function than baseline methods such as Deep Sets and SetTransformers.

While the above introduction situates our research and establishes the setting of our paper in the context of previous related work, our relation to still **other related work** is further explored in our first Appendix in §A. The appendices continue (starting at §B) offering further details of DSPN learning via the GPC-style peripetal loss.

2 Deep Submodular Peripetal Networks

A deep submodular peripetal network (DSPN) is an expressive trainable parametric nonsmooth subdifferentiable submodular function. A DSPN has three stages: (1) a pillar stage; (2) a submodular-preserving permutation-invariant aggregation stage; and (3) a roof stage. When considered together, these three stages resemble an ancient Greek or Roman “peripetal” temple as shown in Figures 11 and 10. In this paper, all DSPNs are also monotone non-decreasing and normalized (see §B). As a set function $f : 2^V \rightarrow \mathbb{R}_+$, a DSPN maps any subset $A \subseteq V$ to a non-negative real number. We consider sets as object indices so A might be a set of image indices while $\{x_i : i \in A\}$ are the objects being referred to. Hence, w.l.o.g., $V = [n]$.

The first stage of a DSPN consists of a set of $|A|$ pillars one for each element in a set A that is being evaluated. The number of pillars changes depending on $|A|$ the size of the set A being evaluated. Each pillar is a many-layered deep neural structure $\phi_{w_p} : \mathcal{D}_X \rightarrow \mathbb{R}_+^d$, parameterized by the vector w_p of real values, that maps from an object (from domain \mathcal{D}_X which could be an image, string, etc.)

to a non-negative embedded representation of that object. For any $v \in V$ and object x_v , then $\phi_{w_p}(x_v)$ is a d -dimensional non-negative real-valued vector $(\phi_{w_p}(x_v)_1, \phi_{w_p}(x_v)_2, \dots, \phi_{w_p}(x_v)_d) \in \mathbb{R}_+^d$. The parameters w_p are shared for all objects. Also, $\phi_{w_p}(x_{:})_j \in \mathbb{R}_+^n$ refers, for any $j \in [d]$, to the n -dimensional vector of the j^{th} pillar outputs for all $v \in V$.

The second stage of a DSPN is a submodular preserving and permutation-invariant aggregation. Before describing this generally, we start with a simple example. Each element $\phi_{w_p}(x_a)_j$ of $\phi_{w_p}(x_a)$ is a score for x_a along dimension j and so a non-negative modular set function can be constructed via $m_j(A) = \sum_{a \in A} \phi_{w_p}(x_a)_j$. Such a summation is an aggregator that, along dimension j simply sums up the j^{th} contribution for every object in A . A simple way to convert this to a monotone non-decreasing submodular function composes it with a non-decreasing concave function ψ yielding $h_j(A) = \psi(m_j(A))$ — performing this for all j yields a d -dimensional vector of submodular functions. More generally, any aggregation function \oplus that preserves the submodularity of $h_j(A) = \psi(\oplus_{a \in A} m_j(a))$ would suffice so long as it is also permutation invariant Zaheer et al. [2017] (see Def. 6). For example, with $\oplus = \max$ (i.e., max pooling), the function $\psi(\max_{a \in A} m_j(a))$ is again submodular. We show that there is an expressive infinitely large family of submodular preserving permutation-invariant aggregation operators, taking the form of the weighted matroid rank functions (Def. 5) which are defined based on a matroid $\mathcal{M} = (V, \mathcal{I})$ and a non-negative vector $m \in \mathbb{R}_+^{|V|}$.

Lemma 1 (Permutation Invariance of Weighted Matroid Rank). *The weighted matroid rank function for matroid $\mathcal{M} = (V, \mathcal{I})$ with any non-negative vector $m \in \mathbb{R}_+^{|V|}$ is permutation invariant.*

A proof is in Appendix B. We identify the aggregator \oplus as $\oplus_{a \in A} m_j(a) = \text{rank}_{\mathcal{M}, m_j}(A)$ and produce a new submodular function $h_j^{w_p}(A) = \psi(\text{rank}_{\mathcal{M}, \phi_{w_p}(x_{:})_j}(A))$, where the n -dimensional vector $\phi_{w_p}(x_{:})_j$ constitute the weights for the matroid. Depending on the matroid, this yields summation (using a uniform matroid), max-pooling (using a partition matroid), and an unbounded number of others thanks to the flexibility of matroids Oxley [2011]. In theory, this means that the aggregator could also be trained via discrete optimization over the space of discrete matroid structures (in §5, however, our aggregators are fixed up front). The second stage of the DSPN thus aggregates the modular outputs of the first stage into a resulting d -dimensional vector for any set $A \subseteq V$, namely $h_{w_p}(A) = (h_1^{w_p}(A), h_2^{w_p}(A), \dots, h_d^{w_p}(A)) \in \mathbb{R}_+^d$. This can also be viewed as a vector of submodular functions. We presume in this work that each aggregator uses the same matroid and each pillar dimension is used with exactly one matroid, but this can be relaxed leading to a $d' > d$ dimensional space — in other words, many different discrete matroid structures can be used at the same time if so desired.

The third and final “roof” stage of a DSPN is a deep submodular function (DSF) Dolhansky and Bilmes [2016]. Deep submodular functions are a nested series of vectors of monotone non-decreasing concave functions composed with each other, layer-after-layer, leading to a final single scalar output. Each layer contained in a DSF has non-negative weight values which assures the DSF is submodular. It was shown in Bilmes and Bai [2017] that the family of submodular functions expressible by DSFs strictly increase with depth. DSFs are also trainable using gradient-based methods analogous to how any deep neural network can be trained. A DSF is defined as a set function, but we utilize the “root”² Bilmes and Bai [2017] multivariate multi-layered concave function $\psi_{w_r} : \mathbb{R}^d \rightarrow \mathbb{R}_+$ of a DSF in this work. The final stage of the DSPN composes the output of the second stage with this final DSF via $f_w(A) = \psi_{w_r}(h_{w_p}(A))$ where $w = (w_p, w_r)$ constitute all the learnable continuous parameters of the DSPN (assuming the discrete parameters, such as the matroid structure, is fixed). While the roof parameters w_r must be positive, the pillar parameters w_p are free, but the pillar must produce non-negative outputs.

Theorem 2 (A DSPN is monotone non-decreasing submodular). *Any DSPN $f_w(A) = \psi_{w_r}(h_{w_p}(A))$ so defined is guaranteed to be monotone non-decreasing submodular for all valid values of w .*

The proof of Theorem 2 is found in Appendix §D. We immediately have the following corollary.

Corollary 3 (Submodular Preservation of Weighted Matroid Rank Aggregators). *Any weighted matroid rank function for matroid $\mathcal{M} = (V, \mathcal{I})$ with any non-negative vector $m \in \mathbb{R}_+^{|V|}$, when used as an aggregator in a DSPN, will be submodularity preserving.*

²“root” here is distinct from “roof”.

Clearly there is a strong relationship between DSPNs and Deep Sets Zaheer et al. [2017]. In fact any DSPNs is a special case of a Deep Set, but there is an important distinction, namely that a DSPN is assuredly submodular. It may seem like this would restrict the family of aggregation functions available but, as shown above, there are in theory an unbounded number of aggregators to study. Training a DSPN also preserves submodularity simply by ensuring w_t remains positive which can be achieved using projected gradient descent (the positive orthant is one of the easiest of the constraints to maintain). A deep set, when trained, can easily lose the submodular property, something we demonstrate in §5, rendering the deep set inapplicable when submodularity is required. Also, as was shown in Bilmes and Bai [2017], DSFs are already quite expressive, the only known limitation being their inability to express certain matroid rank functions. With a DSPN, however, the aggregator functions immediately eliminate this inability. Hence, it is an open theoretical problem if a DSPN, by varying in parameter w and combinatorial space \mathcal{M} , can represent all possible monotone non-decreasing submodular functions.

3 Peripteral Loss

In this section, we describe a new “peripteral” loss to train a DSPN and simultaneously address how to learn, in a modern machine learning context, from numerically graded pairwise comparisons (GPCs) queryable from a target oracle.

We are given two objects E and M and we assume access to an oracle that when queried provides a numerical score $Score(E, M) \in \mathbb{R}$. As shorthand, we define $\Delta(E|M) = Score(E, M)$. We do not presume it is always possible to optimize over $\Delta(E|M)$. This score, as mentioned above, could come from human annotators giving graded preferences for E vs. M , or could be an expensive process of training a machine learning system separately on data subsets E and M and returning the difference in accuracy on a development set. In the context of DSPN learning, our score comes from the difference of a computationally challenging target submodular function f_t . As an example, f_t could be a facility location function that requires $O(n^2)$ time and memory and is not streaming friendly, where we have $\Delta(E|M) = f_t(E) - f_t(M)$, this being a positive if E is more diverse than M and negative otherwise. Given a collection of E, M pairs (§4), we wish to efficiently transfer knowledge from the oracle target’s graded preferences $\Delta(E|M)$ to the learners graded preferences $\delta_{f_w}(E|M) = f_w(E) - f_w(M)$ by adjusting the parameters w of the learner f_w .

We are inspired by simple binary linear SVMs that learn a binary label $y \in \{+1, -1\}$ using a linear model $\langle \theta, x \rangle$ for input x and a hinge loss $hinge(z) = \max(1 - z, 0)$. We express the loss of a given prediction for x as $hinge(y\langle \theta, x \rangle)$ where $y\langle \theta, x \rangle$ is positive for a correct prediction and negative otherwise, regardless of the sign of y .

Addressing how to measure $\delta_{f_w}(E|M)$ ’s divergence from $\Delta(E|M)$, multiplying the two (as above) would have the same sign benefit as the linear hinge SVM — a positive product indicates the preference for E vs. M is aligned between the oracle and learner. We want more than this, however, since we wish to learn from GPC. Instead, therefore, we measure mismatch via the ratio $\delta_{f_w}(E|M)/\Delta(E|M)$. Immediately, we again have a positive quantity if preferences between oracle and target are aligned, but here grading also matters. A good match makes $\delta_{f_w}(E|M)/\Delta(E|M)$ not only positive but also large. If $\Delta(E|M)$ is large and positive, $\delta_{f_w}(E|M)$ must also be large and positive to make the ratio large and positive, while if $\Delta(E|M)$ is small and positive, $\delta_{f_w}(E|M)$ must also be positive but need not be too large to make the ratio large. A similar property holds when $\Delta(E|M)$ is negative. That is, if $\Delta(E|M)$ is large and negative, then so would $\delta_{f_w}(E|M)$ need to be to make the ratio large and positive, while $\Delta(E|M)$ being small and negative allows for $\delta_{f_w}(E|M)$ to be small and negative while ensuring the ratio is large and positive.

On the other hand, a ratio alone is not a good objective to maximize, one big reason being that small changes in the denominator can have disproportionately large effects on the value of the ratio, which can amplify noise and lead to erratic optimization behavior, not to mention $\delta/0$ issues³ which we address further below. Ideally, we could find a hinge-like loss that will penalize small ratios and reward large ratios. Consider the following:

$$\mathcal{L}_\Delta(\delta) = |\Delta| \log(1 + \exp(1 - \frac{\delta}{\Delta})) \quad (1)$$

³In the sequel, we use Δ and δ where the E, M pair is implicit.

Here, if Δ is (very) positive, then δ must also be (very) positive to produce a small loss. If Δ is (very) negative then so also must δ be to produce a small loss. The absolute value of Δ determines how non-smooth the loss is so we include an outer pre-multiplication by $|\Delta|$ to ensure the slope of the loss, as a function of δ , asymptotes to negative one (or one when Δ is negative) in the penalty region, analogous to hinge loss, and thus produces numerically stable gradients. Also analogous to hinge, we add an extra “1” within the $\exp()$ function as a form of margin confidence, analogous to hinge loss that, as with SVMs, expresses a distance between the decision boundary and the support vectors. Plots of $\mathcal{L}_\Delta(\delta)$ are shown in Fig. 7 in Appendix F which also discusses the smoothness of $\mathcal{L}_\Delta(\delta)$ via its gradients.

Having established the “mother” loss $\mathcal{L}_\Delta(\delta)$ we augment it with additional hyperparameters in way that produces smoother and more stable and convergent optimization. Firstly, rather than a requiring a margin of one, we introduce a hyperparameter τ to express this margin whose default value is $\tau = 1$. Second, since the units of the oracle target might be different than the units of the learner, we introduce a unit adjustment parameter κ that scales Δ . We also introduce an anti-smoothness parameter $\beta > 0$ (smaller β means smoother loss) to further optionally smooth the transition between the linearly increasing loss region and the zero-loss region of δ . Lastly, if Δ gets small, to avoid finite-precision numerical problems, we add a small signed value $\epsilon \operatorname{sgn}(\Delta)$ for $\epsilon \geq 0$ which slightly pushes the denominator away from zero depending on the sign of Δ . This yields $\mathcal{L}_{\Delta; \beta, \tau, \kappa, \epsilon}(\delta)$ which is defined as:

$$\mathcal{L}_{\Delta; \beta, \tau, \kappa, \epsilon}(\delta) \triangleq \frac{|\kappa\Delta + \epsilon \operatorname{sgn} \Delta|}{\beta} \log(1 + \exp(\beta(\tau - \frac{\delta}{\kappa\Delta + \epsilon \operatorname{sgn} \Delta}))) \quad (2)$$

There is one last issue with the above we must address, namely when Δ becomes extremely small or zero. This is perfectly reasonable since it expresses the oracle’s indifference to E vs. M . We address this with a tanh-based “gating” function that detects when Δ is very small and gates towards a secondary loss that penalizes the absolute value of δ . The final peripetal loss $\mathcal{L}_{\Delta; \alpha, \beta, \tau, \kappa, \epsilon}(\delta)$ thus has the form:

$$\mathcal{L}_{\Delta; \alpha, \beta, \tau, \kappa, \epsilon}(\delta) \triangleq \tanh\left(\frac{\alpha}{|\kappa\Delta|}\right)|\delta| + \left(1 - \tanh\left(\frac{\alpha}{|\kappa\Delta|}\right)\right)\mathcal{L}_{\Delta; \beta, \tau, \kappa, \epsilon}(\delta) \quad (3)$$

The rate of the gating is determined by $\alpha \geq 0$, and since $\frac{\alpha}{|\kappa\Delta|} \geq 0$, the gate switches to the absolute value $|\delta|$ whenever Δ gets very small. Thus if the oracle target is indifferent to E vs. M this encourages the learner also to be indifferent. Despite these hyperparameters, the loss gradient is still independent of the margin and β making it useful for fine-tuning a learning rate (see §F) for gradient-based learning.

Comparing with standard contrastive losses and deep metric learning Balestrieri et al. [2023], a peripetal loss on $\delta_{f_w}(E|M) = f_w(E) - f_w(M)$ can be seen as a high-order self-normalizing by Δ generalization of triplet loss Weinberger and Saul [2009] if E is a heterogeneous and M a homogeneous set of objects. We recover aspects of a triplet loss if we set $E = \{v, v^-\}$ and $M = \{v, v^+\}$ where M is the positive pair (close and homogeneous) while E is the negative pair (distant from each other and thus a diverse pair). With $|E| > 2$ and $|M| > 2$, we naturally represent high order relationships amongst both the positive group M and the disperse group E . We remind the reader that while our peripetal loss could be used for GPC-style contrastive training for representation learning or for RLHF, our experiments in this paper in §5 focus on the submodular learning problem.

3.1 Augmented Loss for Augmented Data

Data augmentation is frequently used to improve the generalization of neural networks. Since augmented images represent the same knowledge in principle, they should have the same submodular valuation and also should be considered redundant by any learnt submodular function. Given a set E of images, let E' represent a same-size set of augmented images generated after augmenting each image $e \in E$. This means any learnt model f_w should have $f_w(E) = f_w(E')$ and $\forall e \in E$, $f_w(e) = f_w(e')$. To ensure this is the case, we use an augmentation regularizer $\mathcal{L}_{\text{aug}}(f_w; E, E')$ defined as follows:

$$\mathcal{L}_{\text{aug}}(f_w; E, E') = \lambda_1(f_w(E) - f_w(E'))^2 + \frac{\lambda_2}{|E|} \sum_{e \in E} (f_w(e) - f_w(e'))^2 \quad (4)$$

Since augmented images represent the same information, the submodular gain of augmented images relative to non-augmented images should be small or zero meaning $f_w(E|E') = f_w(E'|E) = 0$ and $\forall e \in E, f_w(e|e') = f_w(e'|e) = 0$. To encourage this, we use an redundancy regularizer $\mathcal{L}_{\text{redn}}(f_w; E, E')$ defined as follows:

$$\mathcal{L}_{\text{redn}}(f_w; E, E') = \lambda_3(f_w(E|E')^2 + f_w(E'|E)^2) + \frac{\lambda_4}{|E|} \sum_{e \in E} (f_w(e|e')^2 + f_w(e'|e)^2) \quad (5)$$

In the above, we square all quantities to provide an extra penalty to larger values, while as quantities such as $f_w(E|E')$ approach zero, we diminish the penalty.

3.2 Final Loss

With all of the above individual loss components described, the final total loss $\mathcal{L}_{\text{tot}}(f_w; \Delta(E|M), \delta_{f_w}(E|M))$ for an E, M pair becomes:

$$\begin{aligned} \mathcal{L}_{\text{tot}}(f_w; \Delta(E|M), \delta_{f_w}(E|M)) &= \mathcal{L}_{\Delta(E|M); \alpha, \beta, \tau, \kappa, \varepsilon}(\delta_{f_w}(E|M)) + \mathcal{L}_{\text{aug}}(f_w; E \cup M, E' \cup M') \\ &\quad + \mathcal{L}_{\text{redn}}(f_w; E, E') + \mathcal{L}_{\text{redn}}(f_w; M, M') \end{aligned} \quad (6)$$

With a dataset $\mathcal{D} = \{(E_i, M_i)\}_{i=1}^N$ of pairs, the total risk is:

$$\hat{\mathcal{R}}(w; \mathcal{D}) = \frac{1}{N} \sum_{i \in [N]} \mathcal{L}_{\text{tot}}(f_w; \Delta(E_i|M_i), \delta_{f_w}(E_i|M_i)). \quad (7)$$

4 Sampling (E,M) Pairs

Training a DSPN via the peripetal loss requires a dataset $\mathcal{D} = \{(E_i, M_i)\}_{i=1}^N$ of pairs of sets to be contrasted with each other where each $E_i, M_i \subseteq V$. Since the DSPN starts with the pillar stage, the learnt model can then be tested on samples that are outside of V as we do in §5. Still, exhaustively training on all pairs of subsets from V is intractable. Therefore, the pairing strategy used to incorporate the sampled sets is a critical component in our dataset construction. We thus propose several practical, both passive and active, sampling strategies to efficiently sample from this combinatorial space. The passive strategies are heuristic-based, while the active strategies are dependent on either the DSPN as it is being learnt or optionally the target function if it is possible to optimize. While we describe an outline of these strategies here, appendix E offers further discussion and analysis.

Passive Sampling: If we assume the maximum set size to be K so that $|E| \leq K$ and $|M| \leq K$ and a training dataset to have C classes or clusters, we may generate E, M pairs in two ways. In **Style-I**, we sample a homogeneous set of size K from a randomly chosen single class and a heterogeneous set of size K randomly over the full dataset. In **Style-II**, we first choose a random set of $C' \leq C$ classes, where C' is chosen uniformly at random over $[C]$, and (if $C' < C$) subselect from the ground set a set $V_{C'} \subseteq V$ containing only those samples corresponding to those C' classes. To choose an E set, we perform K-Means clustering on $V_{C'}$, and pick the sample closest to each cluster mean to construct our set. To build an M set, we choose one sample for each class/cluster in $V_{C'}$ and then add its $\lfloor K/C' \rfloor - 1$ nearest neighbors. Importantly, the E and M sets in each pair sampled with **Style-II** are much more difficult to distinguish than **Style-I**. We also note that these sampling strategies are imperfect, so the supposedly heterogeneous E set may not truly be heterogeneous in relation to its homogeneous counterpart M . However, as discussed in §E, the peripetal loss allows us to train the DSPN parameters even if the set pairs are imperfectly labeled since the oracle target just flips the sign of its preference.

Active Sampling: Sets selected by the passive strategies are independent of both the learner and the target function. Thus, due to the combinatorial nature of the problem, there may be a discrepancy between what sets are valued highly by the DSPN and/or the target. This leads us to employ *actively sampled sets* obtained through two approaches. We refer to the first approach as **DSPN Feedback**, which obtains sets by maximizing or minimizing the DSPN as it is being learnt. As DSPN is submodular, we may optimize it over either full ground set V or a class-restricted ground set to get high-valued subsets, where the greedy algorithm can be used for maximization Nemhauser et al. [1978] and submodular minimization Fujishige [2005] can be used to find the homogeneous sets (although in practice, submodular minimization heuristics suffice). We refer to the second approach

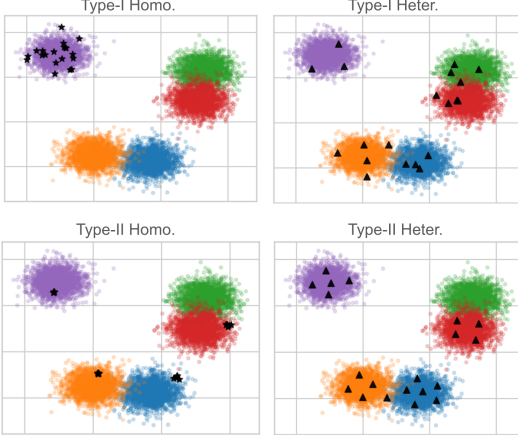


Figure 1: **Passive Sets.** We consider a simple 2D ground set with 5 clusters/classes, as indicated by the colors. The various types of passively sampled sets are depicted (discussed in section 4). Type-I homogeneous sets are randomly sampled from a single class, while Type-I heterogeneous sets are sampled from the full ground set. Meanwhile, Type-II restricts the ground set to a subset of classes and samples “clumps” from each of the sampled classes to construct the homogeneous set, and diverse sets from each class to create the heterogeneous sets. Intuitively, using Type-I/II allows the learnt DSPN to model intraclass/interclass respectively.

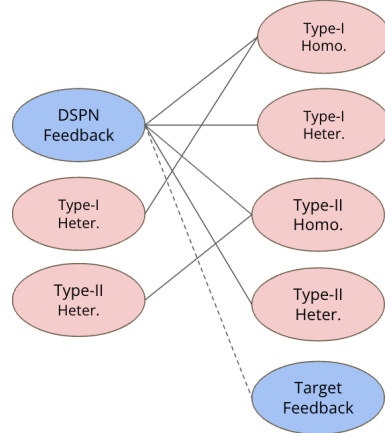


Figure 2: **Set Pairing.** We actively sample sets by optimizing the DSPN as it is being learnt or optionally the target function. The depicted graph demonstrates how the actively sampled sets are integrated into $\mathcal{D} = \{(E_i, M_i)\}_i^N$. The red/blue vertices refer to passively/actively sampled sets. An edge between two vertices indicates that sets from the categories denoted by the vertices are used to create (E, M) pairs to train the DSPN.

as **Target Feedback**, where we obtain sets by maximizing the target. The latter approach is only applicable when the target is optimizable (e.g., submodular), which would not be the case with a human oracle. While we do test “Target Feedback” below, our experiments in §5.3 show that it is not necessary for good performance, which portends well for our framework to be used in other GPC contexts (e.g., RLHF reward learning). Thus, while the E, M pair generation strategies mentioned here are specific to DSPN learning, our peripetal loss could be used to train any deep set or other neural network given access to graded oracle preferences, thus yielding a general purpose GPC-style learning procedure.

We now provide a 2D visual example of what passive sets look like in a simplified setting, shown in fig. 1 as well as illustrate the method in which sets are paired in fig. 2. Lastly, in fig. 3 we provide the structure of a DSPN as well as the control flow of how a DSPN is trained; please refer to appendix G for more details.

5 Experiments

We evaluate the effectiveness of our framework by learning a DSPN that can emulate a costly target oracle facility location function. We assert that DSPN training is deemed successful if the subsets recovered by maximizing the learnt DSPN are (1) assigned high values by the target function (§5.1); (2) are usable for some downstream task such as training a predictive model (§5.2). See §H for hyperparameter details.

Datasets: We consider four image classification datasets: Imagenette, Imagewoof, CIFAR100, and Imagenet100. Imagenette, Imagewoof, and Imagenet100 are subsets of Imagenet-1k Russakovsky et al. [2015], where a subset of the original classes is used. Unlike Imagenet100/CIFAR100, Imagenette and Imagewoof have 10 classes.

DSPN Architecture: We use CLIP ViT encoder Radford et al. [2021] for all datasets to get the embeddings that are used as inputs to the DSPN pillar. We use a 2-layer network as the pillar (ϕ_{w_p}); for DSPN roof (ψ_{w_r}) we use a 2-layered DSF for Imagenette/Imagewoof and 1-layered DSF for CIFAR100/Imagenet100. We use multiple concave activation functions, i.e., all of $\sigma(x) \in$

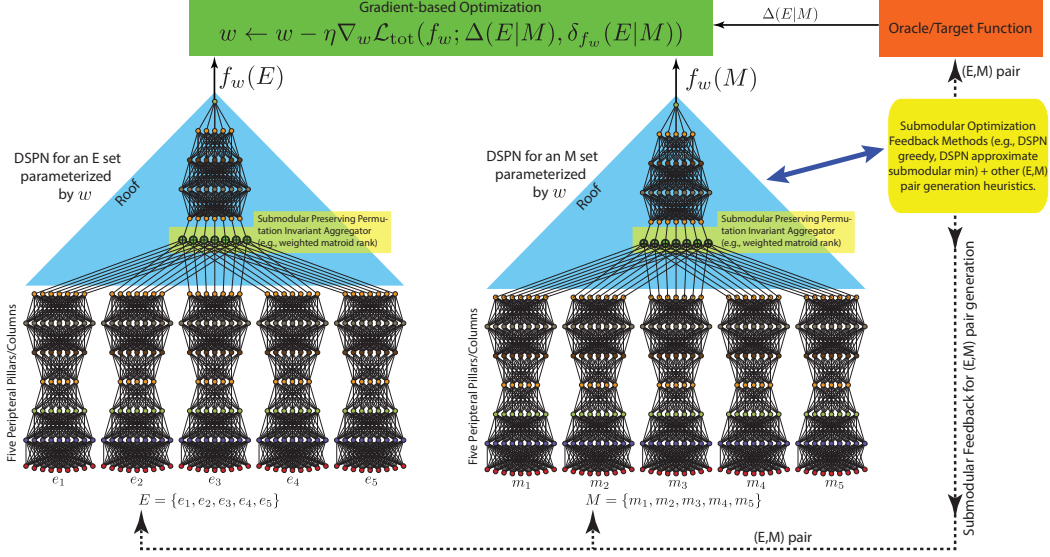


Figure 3: The structure of a DSPN as well as the control flow of how a DSPN is trained; parameters are shared between the DSPNs processing E and M sets.

$\{x, x^{0.5}, \ln(1 + x), \tanh(x), 1 - e^{-x}\}$ in every layer of the roof (ensuring $w_r \geq 0$ during training) and thus allow the training procedure to decide between them.

Training and Evaluation: We train up to sets of size $|E|, |M| \leq 100$ for all datasets. However, we show that we generalize beyond this size even on held-out data. Given ground set V , we construct pairs (E, M) both passively and actively, as discussed earlier. Please refer to §G for the details on training. For the target oracle, we use a facility location function with similarity instantiated using a radial basis function kernel with a tuned kernel width. During the evaluation, both learned set functions and target oracle use a held-out ground set V' of images, that is, $V' \cap V = \emptyset$.

5.1 Transfer from Target to Learner

We demonstrate that the target FL assigns high values to summaries that are generated by the DSPN in Figure 4. Specifically, we determine if S is a good quality set if it has a high normalized FL evaluation $\frac{f_t(S)}{f_t(S_{FL})}$, where f_t is the target FL and S_t is the set generated by applying cardinality constrained greedy maximization to the target FL. Therefore, we compare different DSPN models based on the normalized FL evaluation that their maximizers attain. We compare DSPN models trained with three different losses: the peripteral loss, the contrastive max-margin style structured prediction loss Taskar et al. [2005], and a regression loss (shown as *DSPN (peripteral)*, *DSPN (margin)* and *DSPN (regression)* respectively in Figure 4). Please refer appendix H for the definition of baseline losses (Equations 28 and 29). We also compare against randomly generated sets, which are denoted as *Random*. From this set of experiments, we find that the DSPN trained with the peripteral loss consistently outperforms all other baselines across different summary sizes (budgets) and datasets. Interestingly, the DSPN outperforms random even on budgets greater than 100, despite never having encountered such subsets during training. This provides evidence that the peripteral loss is the loss of choice for training DSPNs.

5.2 Application to Experimental Design

In the context of machine learning, experimental design involves selecting a subset of unlabeled examples from a large pool for labeling to create a training set Pronzato and Pázman [2013]. In this section, we evaluate the performance of a learnt DSPN based on how well a simple linear model generalizes when trained on a training set that was chosen by a DSPN. We consider an *offline setting* where we assume the full unlabeled pool is available and an *online setting* where the unlabeled pool is presented to the model in a non-iid stream. To test the robustness of our framework to real-world

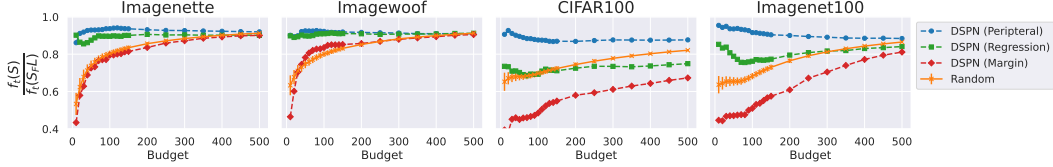


Figure 4: **Transfer.** We evaluate the target function on sets generated by running greedy max on DSPN’s trained with various losses, as well as randomly generated sets. We demonstrate that the DSPN trained with the peripetal loss generates sets that achieve the highest normalized FL evaluations across budgets and datasets.

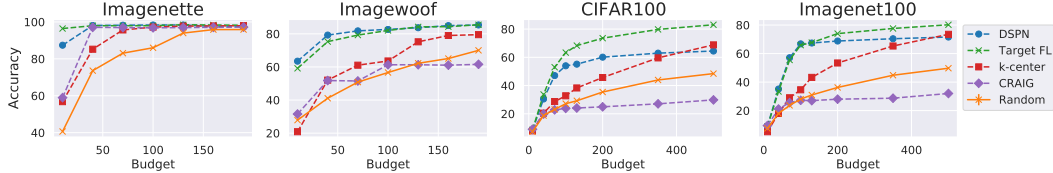


Figure 5: **Offline Experimental Design.** We compare different summarization procedures, and assess them based on the test accuracy that a linear model attains upon being trained on the summary. We find that maximizing the learnt DSPN generates high quality datasets, outperforming existing summarization techniques such as CRAIG and k-centers. In many cases, the DSPN approaches the Target FL even though the latter is aware of the duplicates present in the data.

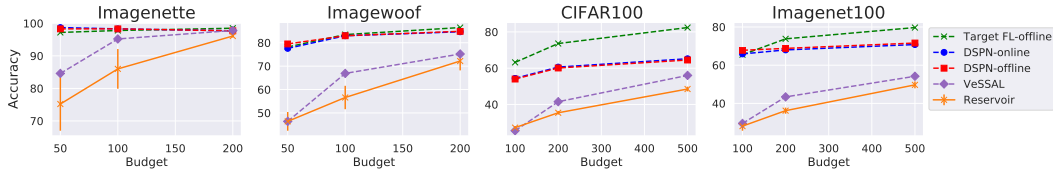


Figure 6: **Online Experimental Design.** The performance of a linear probe, trained based on a subset selected by an algorithm that does not use labels, is reported at varying budgets. *DSPN-online* achieves far higher performance than other streaming algorithms such as *reservoir sampling* and *VeSSAL* and is performs comparably to offline algorithms.

challenges, we add duplicates such that the ground set is heavily class-imbalanced (the procedure to generate the class-imbalanced set is shown in Appendix H).

Offline Setting: The offline setting assumes that the full unlabeled pool is accessible by the summarization procedure. The results of these experiments are presented in Figure 5. Our approach, denoted as *DSPN* in the figure, applies greedy maximization to the learnt DSPN to generate the summary. We also consider a *cheating* experiment by applying greedy to the target FL after removing duplicates from the ground set; we refer to this approach as *Target FL*. Finally, we consider three baseline summarization procedures, CRAIG Mirzasoleiman et al. [2020], K-centers Sener and Savarese [2017], and random subset selection as done in Okanovic et al. [2024]. We find that the learnt DSPN achieves performance comparable to the target FL in all datasets up to a budget of 100. Beyond that, the difference between DSPN and the Target FL grows but the DSPN continues to generate higher quality than any of the baselines.

Online Setting: We consider an online setting where the data is presented to the model in a non-iid, class-incremental stream, as done in the continual learning literature Lopez-Paz and Ranzato [2017], Chaudhry et al. [2019], Aljundi et al. [2019], Zhou et al. [2023]. Unlike the facility location function which requires the full ground set for evaluation, the DSPN can be maximized in a streaming manner. Thus, we employ the streaming maximization algorithm proposed by Lavania et al. [2020] to maximize the DSPN, due to its effectiveness in real-world settings and its lack of additional memory requirements. This approach is referred to as *DSPN-online* in Figure 6.

We compare our approach against two streaming summarization baselines. The first approach, *reservoir sampling* Vitter [1985], is an algorithm that enables random sampling of a fixed number of items from a data stream as if the sample was drawn from the entire population at once. The second approach, *VeSSAL* Saran et al. [2023], seeks to select samples such that the summary maximizes the

Method	FL Eval	Offline Acc	Online Acc
DSPN	0.92	67.8	65.9
w/o target feedback	0.93	67.7	66.9
w/o feedback	0.83	47.7	30.1
w/o learnt pillar	0.71	39.1	38.0
Deep Set	0.56	9.2	3.5
Set Transformer	0.34	13.8	–

Table 1: *Ablations on Imagenet100*. The importance of including feedback, using learnt features, and enforcing submodularity. “w/o feedback” indicates a DSPN model trained without feedback, while “w/o target feedback” is when the oracle is only queried. For Set Transformer, streaming maximization fails to produce a summary of the required size, therefore, we omit that result. All results are reported at a fixed set size of 100.

determinant of the gram matrix constructed from the model embeddings. We also apply (offline) greedy maximization to the target facility location (*Target FL-offline*) and the learned DSPN (*DSPN-offline*), which serve as upper bounds to what is attainable by streaming DSPN maximization.

In Figure 6, we present quantitative results where a linear model is trained on a given streaming summary after labels have been obtained. We find that *DSPN-online* significantly outperforms the other streaming baselines on all datasets. Surprisingly, *DSPN-offline* and *DSPN-online* achieve similar performance, demonstrating the flexibility of DSPN. *FL-offline* tends to generate the highest quality summaries, but requires access to the full ground set and assumes duplicates can be manually removed.

5.3 Ablations

In Table 1, we provide Imagenet100 results on sets of size 100 that explore the importance of various components of the DSPN. We report three numbers for each ablation: (1) *FL Eval* which corresponds to the normalized FL evaluation discussed in § 5.1 (2) *Offline Acc* which denotes the final accuracy of a linear model in the offline experimental design setting and (3) *Online Acc* denotes the final accuracy of a linear model in the online experimental design setting.

Removing (FL) Feedback: Active selection is obtained by maximizing the DSPN or Target FL during training (denoted as *DSPN feedback* and *Target feedback* respectively). We find that only removing the sets obtained from target feedback has little to no impact on the final performance of the DSPN, suggesting that it is not necessary to optimize the target function. *This shows that our framework can be applied to learn DSPNs even when it is not easy to optimize the target.* However, we find that completely removing Active selection significantly hurts the final DSPN.

Removing Learnable Pillar: We assess the utility of a learnable pillar, by training a DSPN with a frozen pillar. In this case, we attempt to learn the weights of a DSF on random projections of CLIP features. We discover that the DSPN without learnable features significantly underperforms its counterpart. We discuss this further in appendix I.

Removing Submodularity: We study the utility of submodular constraints to learn the target. To this end, we compare DSPN against a Deep Set Zaheer et al. [2017] and SetTransformer Lee et al. [2019] architecture in the third section of table 1. Upon doing so, we discover that the absence of submodularity hampers the performance for all the metrics that we consider, since the greedy algorithm has no guarantees for an arbitrary set function.

6 Conclusion and Future Work

In this paper, we propose DSPNs and methods for training them. Since the computational cost of querying a DSPN is independent of dataset size n , and the training scheme leverages automatically generated (E, M) pairs, our method learns practical submodular functions in a scalable manner. In the future, it may be possible to scale our training framework to massive heterogeneous datasets to

develop foundation DSPNs that have strong *zero-shot summarization* capabilities on a wide array of domains.

We also propose the *peripheral loss* which leverages numerically graded relationships between pairs of objects. In our framework, the graded pairwise preferences are provided from an oracle function and are used to learn a submodular function that captures these relationships. However, the scope of the peripheral loss extends far beyond training DSPNs and has many applications in modern machine learning such as learning a reward model in the context of RLHF.

7 Acknowledgements

We thank Suraj Kothawade, Krishnateja Killamsetty and Rishabh Iyer for several earlier discussions. This work is supported in part by the CONIX Research Center, one of six centers in JUMP, a Semiconductor Research Corporation (SRC) program sponsored by DARPA, NSF Grant Nos. IIS-2106937 and IIS-2148367, and by NIH/NHGRI U01 award HG009395.

Bibliography

Stephen Adams, Tyler Cody, and Peter A Beling. A survey of inverse reinforcement learning. *Artificial Intelligence Review*, 55(6):4307–4346, 2022.

Rahaf Aljundi, Min Lin, Baptiste Goujaud, and Yoshua Bengio. Gradient based sample selection for online continual learning. *arXiv preprint arXiv:1903.08671*, 2019.

Saurabh Arora and Prashant Doshi. A survey of inverse reinforcement learning: Challenges, methods and progress. *Artificial Intelligence*, 297:103500, 2021.

F. Bach. Structured sparsity-inducing norms through submodular functions. In *NIPS*, 2010.

Maria-Florina Balcan and Nicholas JA Harvey. Submodular functions: Learnability, structure, and optimization. *SIAM Journal on Computing*, 47(3):703–754, 2018.

Maria Florina Balcan, Florin Constantin, Satoru Iwata, and Lei Wang. Learning valuation functions. *COLT*, 2011.

Maria-Florina Balcan, Ellen Vitercik, and Colin White. Learning combinatorial functions from pairwise comparisons. In *Conference on Learning Theory*, pages 310–335. PMLR, 2016.

Randall Balestrieri, Mark Ibrahim, Vlad Sobal, Ari Morcos, Shashank Shekhar, Tom Goldstein, Florian Bordes, Adrien Bardes, Gregoire Mialon, Yuandong Tian, et al. A cookbook of self-supervised learning. *arXiv preprint arXiv:2304.12210*, 2023.

Gordon G Bechtel. The analysis of variance and pairwise scaling. *Psychometrika*, 32(1):47–65, 1967.

Gordon G Bechtel. A covariance analysis of multiple paired comparisons. *Psychometrika*, 36(1):35–55, 1971.

Gantavya Bhatt, Yifang Chen, Arnav M. Das, Jifan Zhang, Sang T. Truong, Stephen Mussmann, Yinglun Zhu, Jeffrey Bilmes, Simon S. Du, Kevin Jamieson, Jordan T. Ash, and Robert D. Nowak. An experimental design framework for label-efficient supervised finetuning of large language models, 2024.

Jeff Bilmes. Submodularity in machine learning and artificial intelligence, 2022.

Jeffrey Bilmes and Wenruo Bai. Deep submodular functions. *arXiv preprint arXiv:1701.08939*, 2017.

Ralph Allan Bradley and Milton E Terry. Rank analysis of incomplete block designs: I. the method of paired comparisons. *Biometrika*, 39(3/4):324–345, 1952.

Niv Buchbinder, Moran Feldman, Joseph Naor, and Roy Schwartz. Submodular maximization with cardinality constraints. In *Proceedings of the twenty-fifth annual ACM-SIAM symposium on Discrete algorithms*, pages 1433–1452. SIAM, 2014.

Gruia Calinescu, Chandra Chekuri, Martin Pal, and Jan Vondrák. Maximizing a monotone submodular function subject to a matroid constraint. *SIAM Journal on Computing*, 40(6):1740–1766, 2011.

L Elisa Celis, Amit Deshpande, Tarun Kathuria, and Nisheeth K Vishnoi. How to be fair and diverse? *arXiv preprint arXiv:1610.07183*, 2016.

Arslan Chaudhry, Marc' Aurelio Ranzato, Marcus Rohrbach, and Mohamed Elhoseiny. Efficient lifelong learning with a-gem. In *ICLR*, 2019.

Paul Christiano, Jan Leike, Tom B. Brown, Miljan Martic, Shane Legg, and Dario Amodei. Deep reinforcement learning from human preferences, 2023.

William H Cunningham. Decomposition of submodular functions. *Combinatorica*, 3(1):53–68, 1983.

William H Cunningham. Optimal attack and reinforcement of a network. *Journal of the ACM (JACM)*, 32(3):549–561, 1985.

Abir De and Soumen Chakrabarti. Neural estimation of submodular functions with applications to differentiable subset selection. *Advances in Neural Information Processing Systems*, 35:19537–19552, 2022.

Brian W Dolhansky and Jeff A Bilmes. Deep submodular functions: Definitions and learning. *Advances in Neural Information Processing Systems*, 29, 2016.

Ethan R Elenberg, Rajiv Khanna, Alexandros G Dimakis, and Sahand Negahban. Restricted strong convexity implies weak submodularity. *The Annals of Statistics*, 46(6B):3539–3568, 2018.

Hossein Esfandiari, Amin Karbasi, and Vahab Mirrokni. Adaptivity in adaptive submodularity. In *Conference on Learning Theory*, pages 1823–1846. PMLR, 2021.

Moran Feldman, Amin Karbasi, and Ehsan Kazemi. Do less, get more: Streaming submodular maximization with subsampling. *Advances in Neural Information Processing Systems*, 31, 2018.

Pierre Foret, Ariel Kleiner, Hossein Mobahi, and Behnam Neyshabur. Sharpness-aware minimization for efficiently improving generalization. In *International Conference on Learning Representations*, 2021. URL <https://openreview.net/forum?id=6Tm1mpos1rM>.

Satoru Fujishige. *Submodular functions and optimization*. Elsevier, 2005.

Alireza Ghadimi and Hamid Beigy. Deep submodular network: An application to multi-document summarization. *Expert Systems with Applications*, 152:113392, 2020. ISSN 0957-4174. doi: <https://doi.org/10.1016/j.eswa.2020.113392>. URL <https://www.sciencedirect.com/science/article/pii/S0957417420302165>.

Justin Gilmer, Behrooz Ghorbani, Ankush Garg, Sneha Kudugunta, Behnam Neyshabur, David Cardoze, George Dahl, Zachary Nado, and Orhan Firat. A loss curvature perspective on training instability in deep learning. *arXiv preprint arXiv:2110.04369*, 2021.

Michel X Goemans, Nicholas JA Harvey, Satoru Iwata, and Vahab Mirrokni. Approximating submodular functions everywhere. In *Proceedings of the twentieth annual ACM-SIAM symposium on Discrete algorithms*, pages 535–544. SIAM, 2009.

Daniel Golovin and Andreas Krause. Adaptive submodularity: A new approach to active learning and stochastic optimization. In *Proceedings of the 23rd Annual Conference on Learning Theory (COLT)*, 2010.

Joy Paul Guilford. Psychometric methods. 1954.

Andrew Guillory and Jeff A Bilmes. Online submodular set cover, ranking, and repeated active learning. *Advances in neural information processing systems*, 24, 2011.

Michael U Gutmann and Aapo Hyvärinen. Noise-contrastive estimation of unnormalized statistical models, with applications to natural image statistics. *Journal of machine learning research*, 13(2), 2012.

Michael Gygli, Helmut Grabner, and Luc Van Gool. Video summarization by learning submodular mixtures of objectives. In *Proceedings of the IEEE Conference on Computer Vision and Pattern Recognition (CVPR)*, June 2015.

Christopher Harshaw, Ehsan Kazemi, Moran Feldman, and Amin Karbasi. The power of subsampling in submodular maximization. *Mathematics of Operations Research*, 47(2):1365–1393, 2022.

Max Horn, Michael Moor, Christian Bock, Bastian Rieck, and Karsten Borgwardt. Set functions for time series. In *International Conference on Machine Learning*, pages 4353–4363. PMLR, 2020.

Rishabh Iyer, Stefanie Jegelka, and Jeff Bilmes. Fast semidifferential-based submodular function optimization. In *International Conference on Machine Learning*, pages 855–863. PMLR, 2013.

Rishabh K Iyer and Jeff A Bilmes. Submodular optimization with submodular cover and submodular knapsack constraints. *Advances in neural information processing systems*, 26, 2013.

Stefanie Jegelka and Jeff Bilmes. Submodularity beyond submodular energies: coupling edges in graph cuts. In *CVPR 2011*, pages 1897–1904. IEEE, 2011.

Ehsan Kazemi, Shervin Minaee, Moran Feldman, and Amin Karbasi. Regularized submodular maximization at scale. In *International Conference on Machine Learning*, pages 5356–5366. PMLR, 2021.

Krishnateja Killamsetty, Sivasubramanian Durga, Ganesh Ramakrishnan, Abir De, and Rishabh Iyer. Grad-match: Gradient matching based data subset selection for efficient deep model training. In *International Conference on Machine Learning*, pages 5464–5474. PMLR, 2021a.

Krishnateja Killamsetty, Durga Sivasubramanian, Ganesh Ramakrishnan, and Rishabh Iyer. Glister: Generalization based data subset selection for efficient and robust learning. In *Proceedings of the AAAI Conference on Artificial Intelligence*, volume 35, pages 8110–8118, 2021b.

Minyoung Kim. Differentiable expectation-maximization for set representation learning. In *International Conference on Learning Representations*, 2022. URL <https://openreview.net/forum?id=MXdFBmHT4C>.

Diederik P Kingma and Jimmy Ba. Adam: A method for stochastic optimization. *arXiv preprint arXiv:1412.6980*, 2014.

Pang Wei Koh, Thao Nguyen, Yew Siang Tang, Stephen Mussmann, Emma Pierson, Been Kim, and Percy Liang. Concept bottleneck models. In *International conference on machine learning*, pages 5338–5348. PMLR, 2020.

Suraj Kothawade, Nathan Beck, Krishnateja Killamsetty, and Rishabh Iyer. Similar: Submodular information measures based active learning in realistic scenarios, 2021.

Alex Kulesza, Ben Taskar, et al. Determinantal point processes for machine learning. *Foundations and Trends® in Machine Learning*, 5(2–3):123–286, 2012.

Chandrashekhar Lavania and Jeff Bilmes. *Auto-Summarization: A Step Towards Unsupervised Learning of a Submodular Mixture*, pages 396–404. SIAM International Conference on Data Mining, 2019. doi: 10.1137/1.9781611975673.45. URL <https://pubs.siam.org/doi/abs/10.1137/1.9781611975673.45>.

Chandrashekhar Lavania, Kai Wei, Rishabh Iyer, and Jeff Bilmes. *A Practical Online Framework for Extracting Running Video Summaries under a Fixed Memory Budget*, pages 226–234. SIAM International Conference on Data Mining (SDM), 2020. doi: 10.1137/1.9781611976700.26. URL <https://pubs.siam.org/doi/abs/10.1137/1.9781611976700.26>.

Eugene Lawler. *Combinatorial optimization: networks and matroids*. Holt, Rinehart, and Winston, 1976.

Jon Lee, Vahab S Mirrokni, Viswanath Nagarajan, and Maxim Sviridenko. Non-monotone submodular maximization under matroid and knapsack constraints. In *Proceedings of the forty-first annual ACM symposium on Theory of computing*, pages 323–332, 2009.

Juho Lee, Yoonho Lee, Jungtaek Kim, Adam Kosiorek, Seungjin Choi, and Yee Whye Teh. Set transformer: A framework for attention-based permutation-invariant neural networks. In *International conference on machine learning*, pages 3744–3753. PMLR, 2019.

Jure Leskovec, Andreas Krause, Carlos Guestrin, Christos Faloutsos, Jeanne VanBriesen, and Natalie Glance. Cost-effective outbreak detection in networks. In *Proceedings of the 13th ACM SIGKDD international conference on Knowledge discovery and data mining*, pages 420–429, 2007.

H. Lin and J. Bilmes. How to select a good training-data subset for transcription: Submodular active selection for sequences. In "*Proc. Annual Conference of the International Speech Communication Association (INTERSPEECH)*", 2009.

H. Lin and J. Bilmes. An application of the submodular principal partition to training data subset selection. In *NIPS workshop on Discrete Optimization in Machine Learning*, 2010.

Hui Lin and Jeff Bilmes. A class of submodular functions for document summarization. In *Proceedings of the 49th annual meeting of the association for computational linguistics: human language technologies*, pages 510–520, 2011.

Hui Lin and Jeff A Bilmes. Learning mixtures of submodular shells with application to document summarization. *arXiv preprint arXiv:1210.4871*, 2012.

Harriet Lingel, Paul Bürkner, Klaus Melchers, and Niklas Schulte. Measuring personality when stakes are high: Are graded paired comparisons a more reliable alternative to traditional forced-choice methods? 12 2022. doi: 10.31234/osf.io/8rt3j. PsyArXiv Preprints, Manuscript in press.

Yuzong Liu, Kai Wei, Katrin Kirchhoff, Yisong Song, and Jeff Bilmes. Submodular feature selection for high-dimensional acoustic score spaces. In *2013 IEEE International Conference on Acoustics, Speech and Signal Processing*, pages 7184–7188. IEEE, 2013.

David Lopez-Paz and Marc' Aurelio Ranzato. Gradient episodic memory for continual learning. In I. Guyon, U. V. Luxburg, S. Bengio, H. Wallach, R. Fergus, S. Vishwanathan, and R. Garnett, editors, *Advances in Neural Information Processing Systems*, volume 30. Curran Associates, Inc., 2017.

László Lovász. Matroid matching and some applications. *Journal of Combinatorial Theory, Series B*, 28(2):208–236, 1980.

R Duncan Luce. *Individual choice behavior: A theoretical analysis*. Wiley, 1959.

Zelda Mariet, Mike Gartrell, and Suvrit Sra. Learning determinantal point processes by corrective negative sampling. In *The 22nd International Conference on Artificial Intelligence and Statistics*, pages 2251–2260. PMLR, 2019.

Grégoire Mialon, Dexiong Chen, Alexandre d’Aspremont, and Julien Mairal. A trainable optimal transport embedding for feature aggregation and its relationship to attention. *arXiv preprint arXiv:2006.12065*, 2020.

Michel Minoux. Accelerated greedy algorithms for maximizing submodular set functions. In *Optimization Techniques: Proceedings of the 8th IFIP Conference on Optimization Techniques Würzburg, September 5–9, 1977*, pages 234–243. Springer, 2005.

Baharan Mirzasoleiman, Amin Karbasi, Rik Sarkar, and Andreas Krause. Distributed submodular maximization. *The Journal of Machine Learning Research*, 17(1):8330–8373, 2016.

Baharan Mirzasoleiman, Jeff Bilmes, and Jure Leskovec. Coresets for data-efficient training of machine learning models. In *International Conference on Machine Learning*, pages 6950–6960. PMLR, 2020.

Marko Mitrovic, Ehsan Kazemi, Morteza Zadimoghaddam, and Amin Karbasi. Data summarization at scale: A two-stage submodular approach. In *International Conference on Machine Learning*, pages 3596–3605. PMLR, 2018.

Marko Mitrovic, Ehsan Kazemi, Moran Feldman, Andreas Krause, and Amin Karbasi. Adaptive sequence submodularity. *Advances in Neural Information Processing Systems*, 32, 2019.

George L Nemhauser, Laurence A Wolsey, and Marshall L Fisher. An analysis of approximations for maximizing submodular set functions—i. *Mathematical programming*, 14:265–294, 1978.

JC Nunnally and IH Bernstein. Psychometric theory third edition. mcgraw-hili. Inc. <https://doi.org/34567890> *DOCmoC*, 998765, 1994.

Patrik Okanovic, Roger Waleffe, Vasilis Mageirakos, Konstantinos E Nikolakakis, Amin Karbasi, Dionysis Kalogerias, Nezihe Merve Gürel, and Theodoros Rekatsinas. Repeated random sampling for minimizing the time-to-accuracy of learning. *Openreview*, 2024. URL <https://openreview.net/forum?id=JnRStoIuTe>.

Long Ouyang, Jeffrey Wu, Xu Jiang, Diogo Almeida, Carroll Wainwright, Pamela Mishkin, Chong Zhang, Sandhini Agarwal, Katarina Slama, Alex Ray, et al. Training language models to follow instructions with human feedback. *Advances in Neural Information Processing Systems*, 35: 27730–27744, 2022.

J.G. Oxley. *Matroid Theory: Second Edition*. Oxford University Press, 2011.

Adam Paszke, Sam Gross, Francisco Massa, Adam Lerer, James Bradbury, Gregory Chanan, Trevor Killeen, Zeming Lin, Natalia Gimelshein, Luca Antiga, et al. Pytorch: An imperative style, high-performance deep learning library. *Advances in neural information processing systems*, 32, 2019.

Manish Prajapat, Mojmir Mutný, Melanie N Zeilinger, and Andreas Krause. Submodular reinforcement learning. *arXiv preprint arXiv:2307.13372*, 2023.

Luc Pronzato and Andrej Pázman. Design of experiments in nonlinear models. *Lecture notes in statistics*, 212(1), 2013.

Charles R Qi, Hao Su, Kaichun Mo, and Leonidas J Guibas. Pointnet: Deep learning on point sets for 3d classification and segmentation. In *Proceedings of the IEEE conference on computer vision and pattern recognition*, pages 652–660, 2017.

Alec Radford, Jong Wook Kim, Chris Hallacy, Aditya Ramesh, Gabriel Goh, Sandhini Agarwal, Girish Sastry, Amanda Askell, Pamela Mishkin, Jack Clark, Gretchen Krueger, and Ilya Sutskever. Learning transferable visual models from natural language supervision, 2021.

Siamak Ravanbakhsh, Jeff Schneider, and Barnabas Poczos. Equivariance through parameter-sharing. In *International conference on machine learning*, pages 2892–2901. PMLR, 2017.

Olga Russakovsky, Jia Deng, Hao Su, Jonathan Krause, Sanjeev Satheesh, Sean Ma, Zhiheng Huang, Andrej Karpathy, Aditya Khosla, Michael Bernstein, Alexander C. Berg, and Li Fei-Fei. ImageNet Large Scale Visual Recognition Challenge. *International Journal of Computer Vision (IJCV)*, 115 (3):211–252, 2015. doi: 10.1007/s11263-015-0816-y.

Mehraveh Salehi, Amin Karbasi, Dustin Scheinost, and R Todd Constable. A submodular approach to create individualized parcellations of the human brain. In *Medical Image Computing and Computer Assisted Intervention- MICCAI 2017: 20th International Conference, Quebec City, QC, Canada, September 11-13, 2017, Proceedings, Part I* 20, pages 478–485. Springer, 2017.

Akanksha Saran, Safoora Yousefi, Akshay Krishnamurthy, John Langford, and Jordan T. Ash. Streaming active learning with deep neural networks, 2023.

Henry Scheffe. An analysis of variance for paired comparisons. *Journal of the American Statistical Association*, 47(259):381–400, 1952. ISSN 01621459. URL <http://www.jstor.org/stable/2281310>.

Alexander Schrijver. *Combinatorial optimization: polyhedra and efficiency*, volume 24. Springer Verlag, 2003.

Ozan Sener and Silvio Savarese. Active learning for convolutional neural networks: A core-set approach. *arXiv preprint arXiv:1708.00489*, 2017.

Roger N Shepard. Stimulus and response generalization: A stochastic model relating generalization to distance in psychological space. *Psychometrika*, 22(4):325–345, 1957.

D Amnon Silverstein and Joyce E Farrell. Efficient method for paired comparison. *Journal of Electronic Imaging*, 10(2):394–398, 2001.

R. Sipos, P. Shivaswamy, and T. Joachims. Large-margin learning of submodular summarization methods. *arXiv preprint arXiv:1110.2162*, 2011.

Ruben Sipos, Pannaga Shivaswamy, and Thorsten Joachims. Large-margin learning of submodular summarization models. In Walter Daelemans, editor, *Proceedings of the 13th Conference of the European Chapter of the Association for Computational Linguistics*, pages 224–233, Avignon, France, April 2012. Association for Computational Linguistics. URL <https://aclanthology.org/E12-1023>.

Leslie N Smith. Cyclical learning rates for training neural networks. In *2017 IEEE winter conference on applications of computer vision (WACV)*, pages 464–472. IEEE, 2017.

Suraj Srinivas, Kyle Matoba, Himabindu Lakkaraju, and François Fleuret. Efficient training of low-curvature neural networks. In Alice H. Oh, Alekh Agarwal, Danielle Belgrave, and Kyunghyun Cho, editors, *Advances in Neural Information Processing Systems*, 2022. URL <https://openreview.net/forum?id=2B2xIJ299rx>.

Peter Stobbe and Andreas Krause. Efficient minimization of decomposable submodular functions. *Advances in Neural Information Processing Systems*, 23, 2010.

Scott Sussex, Caroline Uhler, and Andreas Krause. Near-optimal multi-perturbation experimental design for causal structure learning. *Advances in Neural Information Processing Systems*, 34: 777–788, 2021.

Ben Taskar, Vassil Chatalbashev, Daphne Koller, and Carlos Guestrin. Learning structured prediction models: A large margin approach. In *Proceedings of the 22nd international conference on Machine learning*, pages 896–903, 2005.

Louis L Thurstone. A law of comparative judgment. *Psychological Review*, 34:273–2786, 1927.

Yonglong Tian, Dilip Krishnan, and Phillip Isola. Contrastive multiview coding. In *Computer Vision–ECCV 2020: 16th European Conference, Glasgow, UK, August 23–28, 2020, Proceedings, Part XI 16*, pages 776–794. Springer, 2020.

Ehsan Tohidi, Rouhollah Amiri, Mario Coutino, David Gesbert, Geert Leus, and Amin Karbasi. Submodularity in action: From machine learning to signal processing applications. *IEEE Signal Processing Magazine*, 37(5):120–133, 2020.

Sebastian Tschiatschek, Rishabh K Iyer, Haochen Wei, and Jeff A Bilmes. Learning mixtures of submodular functions for image collection summarization. *Advances in neural information processing systems*, 27, 2014.

Sebastian Tschiatschek, Aytunc Sahin, and Andreas Krause. Differentiable submodular maximization. *arXiv preprint arXiv:1803.01785*, 2018.

Jeffrey S. Vitter. Random sampling with a reservoir. *ACM Trans. Math. Softw.*, 11(1):37–57, mar 1985. ISSN 0098-3500. doi: 10.1145/3147.3165. URL <https://doi.org/10.1145/3147.3165>.

Yuanhao Wang, Qinghua Liu, and Chi Jin. Is rlhf more difficult than standard rl? a theoretical perspective. In *Thirty-seventh Conference on Neural Information Processing Systems*, 2023.

Kai Wei, Yuzong Liu, Katrin Kirchhoff, and Jeff Bilmes. Unsupervised submodular subset selection for speech data. In *2014 IEEE International Conference on Acoustics, Speech and Signal Processing (ICASSP)*, pages 4107–4111. IEEE, 2014.

Kai Wei, Rishabh Iyer, and Jeff Bilmes. Submodularity in data subset selection and active learning. In *International conference on machine learning*, pages 1954–1963. PMLR, 2015.

Kilian Q Weinberger and Lawrence K Saul. Distance metric learning for large margin nearest neighbor classification. *Journal of machine learning research*, 10(2), 2009.

Christian Wirth, Riad Akour, Gerhard Neumann, Johannes Fürnkranz, et al. A survey of preference-based reinforcement learning methods. *Journal of Machine Learning Research*, 18(136):1–46, 2017.

Manzil Zaheer, Satwik Kottur, Siamak Ravanbakhsh, Barnabas Poczos, Russ R Salakhutdinov, and Alexander J Smola. Deep sets. *Advances in neural information processing systems*, 30, 2017.

Wenhao Zhan, Masatoshi Uehara, Nathan Kallus, Jason D Lee, and Wen Sun. Provable offline reinforcement learning with human feedback. *arXiv preprint arXiv:2305.14816*, 2023.

Yan Zhang, Jonathon Hare, and Adam Prugel-Bennett. Deep set prediction networks. *Advances in Neural Information Processing Systems*, 32, 2019.

Da-Wei Zhou, Qi-Wei Wang, Zhi-Hong Qi, Han-Jia Ye, De-Chuan Zhan, and Ziwei Liu. Deep class-incremental learning: A survey, 2023.

Yuxun Zhou and Costas J Spanos. Causal meets submodular: Subset selection with directed information. *Advances in Neural Information Processing Systems*, 29, 2016.

Banghua Zhu, Jiantao Jiao, and Michael I Jordan. Principled reinforcement learning with human feedback from pairwise or k -wise comparisons. *arXiv preprint arXiv:2301.11270*, 2023.

George Kingsley Zipf. *The psycho-biology of language: An introduction to dynamic philology*. Routledge, 2013.

A Other Related Work

In addition to the previously discussed literature in §1 that addresses learning through pairwise comparison, human preference elicitation, and contrastive learning, this section provides a comprehensive review of both theoretical and empirical studies related to the learning of set functions.

Learning Non-submodular Set functions Recently, there has been a growing focus on leveraging data-driven neural methods for estimating set functions, with practical applications spanning anomaly detection, amortized clustering of mixture models, and point cloud classification Qi et al. [2017]. Common to these applications is the fundamental approach of embedding each element within a set into dense embeddings, followed by permutation-invariant aggregation (set-to-vector transformation), and subsequent integration into a deep neural network Zaheer et al. [2017], Horn et al. [2020], Ravanbakhsh et al. [2017]. The significance of incorporating interaction among set elements has been emphasized by Lee et al. [2019], who argue that conventional aggregations, such as average-pooling, can be interpreted as a specialized form of attention. Consequently, they propose an attention-based architecture known as the set-transformer. Building upon this, Mialon et al. [2020] have made computational enhancements to the attention-based architecture. Lastly, there has been a recent exploration into a probabilistic interpretation of set-to-vector transformations Zhou et al. [2023], Kim [2022], further refining the methodology.

The works mentioned above diverge from our approach for several reasons. Firstly, they primarily focus on supervised learning oracles utilizing static datasets to learn neural parameters, whereas our method draws inspiration from max-margin contrastive learning and employs a dynamically updated dataset. Secondly, these existing works lack architectural and/or optimization constraints ensuring the submodularity of the learned set function, in contrast to our work on learning deep submodular functions, where submodularity is explicitly guaranteed. However, for a comprehensive evaluation against existing literature, we include Deep Sets and Set-Transformer as a baseline for comparison. Thirdly, the set sizes used in these works are much smaller (30 in many experiments) compared to ours which go up to 500. Lastly, the learned set function in these works lacks a clear interpretation associated with extremal—sets that (locally) maximize or minimize the set function. In contrast, our Deep Submodular Function (DSF) yields heterogeneous/homogeneous sets upon maximization/minimization. It is noteworthy that the choice of a submodular function as the inductive bias may not be essential for certain tasks, such as point-cloud classification and amortized clustering of mixture models. However, it proves to be a plausible inductive bias in scenarios where the objective is to count unique characters Zaheer et al. [2017], Zhou et al. [2023], Kim [2022], Lee et al. [2019],

since it can be exactly be expressed as a partition matroid rank function, which lies in the family of deep submodular function.

Beyond neural approaches, one of the previous works Mariet et al. [2019] has also considered learning Determinantal Point Process, or DPPs Kulesza et al. [2012], by learning the $\mathcal{O}(n^2)$ similarity matrix by noise contrastive estimation Gutmann and Hyvärinen [2012]. However, their learning procedure is different from ours, and sampling from a DPP is much more computationally expensive than maximizing a submodular function.

Theoretical Work on Learning Submodular Functions Numerous works have investigated strategies for understanding submodular functions from a theoretical perspective. Goemans et al. [2009] examined the approximation of an oracle for every subset, utilizing a multiplicative approximation approach to approximate the submodular polyhedron of the oracle using Löwner ellipsoids. In contrast, Balcan et al. [2011], Balcan and Harvey [2018] focused on approximating the oracle with high probability on sets sampled from specific distributions (often referred to as Probabilistic Modular Agnostic (PMAC) learning) by transforming the problem into the identification of linear separators. Notably, Balcan and Harvey [2018] demonstrated the impracticality of approximating any arbitrary monotone non-decreasing submodular function to arbitrary closeness under PMAC learning in polynomial queries. Subsequently, Balcan et al. [2016] proposed an algorithm for learning the oracle through pairwise comparisons in polynomial queries. While this work shares theoretical commonalities with ours, it is important to highlight that Balcan et al. [2016] examined set pairs sampled from a static distribution, contrasting with our approach, which involves a dynamically changing distribution of set pairs due to our submodular feedback. Remarkably, across the aforementioned works, the learned functions exhibit a form that can be represented easily using a Deep Submodular Function (DSF), a facet that our work incorporates and explores further.

Neural Estimation of Submodular Functions Since submodular functions have $2^{|V|}$ degrees of freedom, empirical approaches of learning submodular functions restrict the search space to a parametric subclass such as feature-based functions or DSFs. Early data-driven learning techniques use the max-margin structured prediction framework introduced in Taskar et al. [2005], which requires human annotators to manually construct summaries/sets that should be assigned high values by the learnt submodular function Lin and Bilmes [2012], Tschiatschek et al. [2014], Sipos et al. [2012], Gygli et al. [2015], Ghadimi and Beigy [2020]. These approaches have consistently demonstrated that learned coefficients, as opposed to handcrafted ones, result in submodular functions that can generate much higher quality summaries. However, these approaches depend on human-constructed summaries which can be prohibitively expensive to procure at scale. Furthermore, that the features suitable for the feature-based function are *not* learned, unlike our work where we jointly learn features and associated parameters for the submodular function. Despite the empirical success of this framework, these approaches all require sets chosen by humans which are difficult to procure at scale.

More recently, De and Chakrabarti [2022] proposed to estimate a submodular function using recursive composition with a learned concave function, arguing that the lack of a “good” concave function is a weakness of DSF (and only used one concave function in their experiments). In our work, we alleviate this by showing that one can learn a good DSF by training with multiple concave functions simultaneously with varying degrees of saturation. It should also be noted that there is no theoretical discussion if the representation capacity of the function class strictly increases with more recursive steps, unlike DSF, where the capacity strictly increases with additional layers. Furthermore, they learn the parameters in a supervised manner, given the annotated high-valued summaries, unlike our work which does so in a self-supervised fashion. Lastly, the learned modular function for DSF has the interpretation of capturing concepts (appendix I) which is not in their case. Remarkably, it is an interesting extension where one combines the technique proposed in De and Chakrabarti [2022] to learn the concave function jointly with our technique for learning the parameters.

Lavania and Bilmes [2019] proposes an unsupervised framework to learn submodular functions, similar to our work. Their approach involves the maximization of a handcrafted objective function, evaluating the quality of weights through measurements of submodular function properties like curvature and sharpness. Notably, they do not engage in the simultaneous joint learning of features alongside parameters and instead they first train an auto-encoder to get the features. To the best of our knowledge, no existing studies have effectively undertaken the joint learning of submodular function parameters and features, a key aspect of our proposed methodology.

Finally, we note the existence of related work using the same nomenclature, DSPN, introduced by Zhang et al. [2019], which stands for Deep Set Prediction Network. The primary objective of Zhang et al. [2019] is to predict a set based on dense features. In contrast, our research focuses on the development of a deep submodular function (DSF) capable of generating sets through optimization.

B Submodular Functions and Weighted Matroid Rank

Submodular set functions effectively capture notions of diversity and representativeness. Continuing on from §1, it is known that they are useful in machine learning in the context of data subset selection Mirzasoleiman et al. [2020], Killamsetty et al. [2021b,a], Wei et al. [2015], feature selection Liu et al. [2013], summarization Lin and Bilmes [2011], active learning Wei et al. [2015], Kothawade et al. [2021], experimental design Bhatt et al. [2024], more recently in reinforcement learning Prajapat et al. [2023] and several other areas that involve some form of discrete optimization. Submodular functions also appear naturally in many other areas, such as theoretical computer science and statistical physics Tohidi et al. [2020], Bilmes [2022].

Submodular functions are also of interest since they enjoy properties sufficient for efficient optimization. For a ground set of size n , they lie in a cone of dimension 2^n in \mathbb{R}^{2^n} , but can still be minimized exactly without constraints in polynomial time [Fujishige, 2005]. Even though submodular function maximization is NP-hard, it offers a fast constant factor approximation algorithm, for instance in the cardinality-constrained case, greedy results in $1 - 1/e$ guarantee for polymatroid functions [Nemhauser et al., 1978, Minoux, 2005]. Similarly one can give guarantees for other constrained cases such as knapsack constraint or more complicated independence or matroid constraints [Buchbinder et al., 2014, Calinescu et al., 2011, Lee et al., 2009, Iyer and Bilmes, 2013, Iyer et al., 2013].

In this section, we offer a brief primer on submodularity and their relationship to matroid rank.

Any function $f : 2^V \rightarrow \mathbb{R}$ that maps from subsets of some underlying ground set V of size $|V| = n$ is called a discrete set function. For a set function to be *submodular*, it must satisfy the property of diminishing returns. This means that for any $X \subseteq Y \subseteq V$ and any $v \in V \setminus Y$ the gain of adding v to the smaller set is larger than the gain of adding v to the larger set, meaning:

$$f(v|X) \triangleq f(X \cup \{v\}) - f(X) \geq f(Y \cup \{v\}) - f(Y) \triangleq f(v|Y) \quad (8)$$

We use the (conditional) gain notation $f(v|X) \triangleq f(X \cup \{v\}) - f(X)$ regularly in the paper. We also assume also that all submodular functions are monotone non-decreasing (or just monotone), which means that for any $X \subseteq Y$ we have that $f(X) \leq f(Y)$ and non-negative, meaning that $0 \leq f(X)$ for any $X \subseteq V$. We also assume f is normalized so that at the emptyset $f(\emptyset) = 0$. Such normalized monotone non-decreasing submodular functions necessarily are always non-negative, and are commonly referred to as polymatroid functions Bilmes [2022], Cunningham [1983, 1985], Lovász [1980].

If Eqn (8) holds with equality for all sets, then the function is referred to as a *modular* function which implies that f can be equated with a length n vector, that is for all $X \subseteq V$, $f(X) = \sum_{x \in X} f(x)$, which means the vector associated with f is $(f(v) : v \in V) \in \mathbb{R}^n$. We often use simplified notation for modular functions — that is, given a length n vector $m \in \mathbb{R}^n$, we can define the modular function $m : 2^V \rightarrow \mathbb{R}$ as $m(A) = \sum_{a \in A} m(a)$.

If the inequality in Eqn (8) holds in the reverse, meaning

$$f(v|X) \triangleq f(X \cup \{v\}) - f(X) \leq f(Y \cup \{v\}) - f(Y) \triangleq f(v|Y) \quad (9)$$

then the function is known as a *supermodular* function.

For completeness, we note that an equivalent definition of submodularity would say that for any two sets $A, B \subseteq V$, we have that $f(A) + f(B) \geq f(A \cup B) + f(A \cap B)$. It is not hard to show that this and Inequality (8) are identical Bilmes [2022], Fujishige [2005].

Given a finite set V and a set of subsets $\mathcal{I} = \{I_1, I_2, \dots\}$, the pair (V, \mathcal{I}) is known as a set system.

Matroids Lawler [1976], Oxley [2011], Schrijver [2003] are useful algebraic structures that are strongly related to submodular functions [Fujishige, 2005]. Given a finite ground set V of size $|V| = n$, a matroid \mathcal{M} is a set system that consists of the pair (V, \mathcal{I}) where V is said ground set and $\mathcal{I} = \{I_1, I_2, \dots\}$ is a set of subsets of V , meaning $I_i \subseteq V$ for all i . To define matroid \mathcal{M} we say

$\mathcal{M} = (V, \mathcal{I})$. The subsets \mathcal{I} are known as the independent sets (meaning, for any $I \in \mathcal{I}$, I is said to be independent) and they have certain properties that make this the set system interesting and useful. Formally, a matroid is defined as follows:

Definition 4 (Matroid). *Given a ground set V of size $|V| = n$, a matroid $\mathcal{M} = (V, \mathcal{I})$ is a set system where the set of subsets $\mathcal{I} = (I_1, I_2, \dots)$ have the following properties:*

1. $\emptyset \in \mathcal{I}$
2. If $I \in \mathcal{I}$ and $I' \subset I$, then $I' \in \mathcal{I}$
3. For any $I, I' \in \mathcal{I}$ with $|I| < |I'|$, there exists a $v \in I' \setminus I$ such that $I \cup \{v\} \in \mathcal{I}$.

Matroids generalize the algebraic properties of vectors in a vector space, where independence of a set corresponds to sets of vectors that are linearly independent. If we think V as a set of indices of vectors, and $A = \{a_1, a_2, \dots\} \subseteq V$, then the A being independent corresponds to the vectors associated with A being linearly independent. Matroids however capture the algebraic properties of independence and there are valid matroids that can not be representable by any vector space. Note also that the algebraic structure is similar to that of collections of random variables that might or might not be statistically independent.

While there are many types and useful properties of matroids, the rank of a matroid measures the independence of a set based on the largest independent set that it contains, namely

$$\text{rank}_{\mathcal{M}}(A) = \max_{I \in \mathcal{I}} |A \cap I| = \max\{B : B \subseteq A \text{ and } B \in \mathcal{I}\} \quad (10)$$

For any matroid, the rank function is submodular, meaning for any $A, B \subseteq V$, $\text{rank}_{\mathcal{M}}(A) + \text{rank}_{\mathcal{M}}(B) \geq \text{rank}_{\mathcal{M}}(A \cup B) + \text{rank}_{\mathcal{M}}(A \cap B)$. For example, the function $f(A) = \min(|A|, \alpha)$ with integral valued α is a classic concave-composed with modular function (which is thus submodular) but is also the rank function for partition matroid with one partition block and limit of α . A matroid rank function is also a polymatroid function since $\text{rank}_{\mathcal{M}}(\emptyset) = 0$ and $\text{rank}_{\mathcal{M}}(A) \leq \text{rank}_{\mathcal{M}}(B)$ whenever $A \subseteq B$.

A matroid rank functions can be significantly extended when it is associated with a non-negative vector $m \in \mathbb{R}_+^{|V|}$ of length $|V| = n$. With such a vector, one can define a weighted matroid rank function:

Definition 5 (Weighted Matroid Rank Function). *Given a matroid $\mathcal{M} = (V, \mathcal{I})$ and a non-negative vector $m \in \mathbb{R}_+^n$, the weighted matroid rank function for this matroid and vector is defined as:*

$$\text{rank}_{\mathcal{M}, m}(A) = \max_{I \in \mathcal{I}} m(A \cap I) \quad (11)$$

A weighted matroid rank function is still submodular and is still a polymatroid function. In fact, weighted matroid rank functions generalize many much more recognizable functions. Here are several examples.

1. Consider a uniform matroid $M = (V, \mathcal{I})$ where $\mathcal{I} = 2^V$. This means that all 2^n subsets of V are independent in the matroid. Then given non-negative vector $m \in \mathbb{R}_+^{|V|}$, the weighted matroid rank function has the form $\text{rank}_{\mathcal{M}, m}(A) = \sum_{a \in A} m(a)$, thus the weighted matroid rank function is just the modular function m .
2. Consider a one-partition matroid rank function with limit $k = 1$. This is a matroid $M = (V, \mathcal{I})$ where $\mathcal{I} = \{A \subseteq V : |A| = 1\}$, meaning all sets of size one are independent but no other set is independent in the matroid. Given non-negative vector $m \in \mathbb{R}_+^{|V|}$, the weighted matroid rank function has the form $\text{rank}_{\mathcal{M}, m}(A) = \max_{a \in A} m(a)$.
3. The facility location function can be seen as the sum of a weighted matroid rank functions using the same matroid as the previous example but using different weights for each term in the sum. That is, given a similarity matrix $[S]_{ai}$ of non-negative entries, the facility location function has form $f(A) = \sum_{i=1}^n \max_{a \in A} s_{ai}$. Hence, using the same matroid as the previous case, the facility location takes the form $f(A) = \sum_{i=1}^M \text{rank}_{\mathcal{M}, s_{:,i}}(A)$ where $s_{:,i}$ is the i^{th} column of the matrix.

Another interesting (and apparently previously unreported) property of weighted matroid rank functions is that they are always permutation invariant in the same sense as a deep set function Zaheer et al. [2017] is permutation invariant. Firstly, we restate the definition of permutation invariance from Zaheer et al. [2017].

Definition 6 (Permutation Invariance Zaheer et al. [2017]). *A function $f : 2^V \rightarrow \mathbb{R}$ acting on sets is said to be permutation invariant if the function is invariant to the order of objects in the set. That is for any set $A \subseteq V$ with $A = \{a_1, a_2, \dots, a_m\}$, and for any permutation $\pi : A \rightarrow A$, we have that for any set $f(\{a_1, a_2, \dots, a_m\}) = f(\{\pi(a_1), \pi(a_2), \dots, \pi(a_m)\})$.*

Thus, permutation invariance means that the order in which elements are considered or arranged does not affect the outcome of the function that is applied to a set. For the weighted matroid rank function, this means that if we take a subset $A \subseteq V$ and permute its elements, the $\text{rank}_{\mathcal{M}, m}(A)$ stays the same. The reason is because the rank function is concerned only with the elements present in the subset, not the order in which they are listed. Thus, permutation invariance aligns with the properties of matroids as we formalize in the next lemma.

Lemma 1 (Permutation Invariance of Weighted Matroid Rank). *The weighted matroid rank function for matroid $\mathcal{M} = (V, \mathcal{I})$ with any non-negative vector $m \in \mathbb{R}_+^{|V|}$ is permutation invariant.*

Proof. The weighted matroid rank function for matroid $\mathcal{M} = (V, \mathcal{I})$ is defined as

$$\text{rank}_m(A) = \max_{I \in \mathcal{I}} m(A \cap I) = \max_{I \in \mathcal{I}} \sum_{a \in A \cap I} m(a) \quad (12)$$

and since nowhere in this definition are the order of the elements in A used, but rather only a sum over some of the elements as shown on the right hand side of the above, the function is permutation invariant. This also immediately follows given Proposition 7. \square

In fact, this property is true for any submodular function.

Proposition 7. *Submodularity and Permutation Invariance.* *Any submodular set function $f : 2^V \rightarrow \mathbb{R}$ is permutation invariant.*

C Primer on Deep Submodular Functions

Stobbe and Krause [2010] proposed a scalable algorithm for minimizing a class of submodular functions known as *decomposable functions*. In general, given a collection of modular functions, $\{m_i\}_{i=1}^N$ where each $m_i : V \rightarrow \mathbb{R}_+$ and ϕ , a monotone non-decreasing, normalized $\phi(0) = 0$ and non-negative concave function,

$$f(A) = \sum_{i=1}^N \phi(m_i(A))$$

is said to be a “decomposable” function.

In machine learning, objects of interest are often represented by featurizing them into a finite-dimensional vector space. If $U = \{u_1, u_2, \dots, u_{|U|}\}$ indexes the dimensions, then for any example $v \in V$ the modular function $m_U(v) = (m_{u_1}(v), m_{u_2}(v), \dots, m_{u_{|U|}}(v))^T$ represents the features of v . $m_u(v)$ can be interpreted in several ways such as the degree of presence of u – th concept in v similar to concept bottleneck models Koh et al. [2020] or even the count of an n-gram feature Wei et al. [2014], Lin and Bilmes [2011, 2012]. With this nomenclature, we re-define *decomposable* submodular functions as feature-based functions that has the form:

$$f(A) = \sum_{u \in U} w_u \phi_u(m_u(A)), \quad (13)$$

where w represents a non-negative weight for each feature. The gain of adding examples with more of the property represented by feature u diminishes as the set gets larger due to concave composition and the diminishing returns of the concave function. Therefore, intuitively the set $X \subseteq V$ that maximizes the feature-based function would comprise examples that produce a diverse set of features according to the features’ properties.

One issue with the feature-based function happens when there is redundancy between two features u_i and u_j . For instance, if the features are a count of n-grams, and since higher-order n-grams encompass lower-order n-grams, having too many of a certain high-order n-gram would also mean having many of its lower-order n-grams, leading to redundancy (or correlation) in what the features represent. As eq. (13) suggests, feature-based functions treat each feature independently. This motivates a flexible class of submodular functions, known as *Deep submodular functions* or DSFs Bilmes and Bai [2017] which mitigates the problem of redundancy by an additional concave composition followed by weighted aggregation which allows for interaction between sets of redundant features as follows:

$$f(A) = \sum_{s \in S} \omega_s \phi_s \left(\sum_{u \in U} w_{s,u} \phi_u (m_u(A)) \right) \quad (14)$$

Here, $w_{s,u}$ and ω_s are non-negative mixture weights. This naturally leads to a representation resembling neural networks when we iteratively apply a concave function followed by linear aggregation, giving rise to Deep Submodular Functions. $\forall s \in S$, Bilmes and Bai [2017] define $\sum_{u \in U} w_{s,u} \phi_u (m_u(A))$ as meta-features, and in general one can stack more layers of concave composition followed by affine transformations, leading to meta-meta features, and so on. Let L be the total number of layers in a DSF; each meta-feature at layer ℓ of this network is a submodular function, we index them using $U^{(\ell)}$, which means in the example in equation (14) $U = U^{(0)}$ and $S = U^{(1)}$.

$W^{(\ell)} \in \mathbb{R}_+^{|U^{(\ell)}| \times |U^{(\ell-1)}|}$ be the mixture weights at layer ℓ , where for the last layer L we have a uniform weight, which means $W^L \in \mathbb{R}_+^{|U^{(L)}|}$ Concave functions applied at the j -th submodular function of layer ℓ is represented by $\phi_j^{(\ell)}$. To write concave functions in vector form, we define $\Phi_U : \mathbb{R}^{|U|} \rightarrow \mathbb{R}^{|U|}$ such that for any $\mathbf{a} \in \mathbb{R}^{|U|}$ we define $\Phi_U(\mathbf{a})$

$$\Phi_U(\mathbf{a}) \triangleq [\phi_1(\mathbf{a}_1), \phi_2(\mathbf{a}_2), \dots, \phi_{|U|}(\mathbf{a}_{|U|})]^T \quad (15)$$

With the notation above, for $X \subseteq V$, DSF $f(A)$ is defined as following

$$f(A) = W^{(L)} \cdot \Phi_{U^{(L-1)}} \left(W^{(L-1)} \cdot \Phi_{U^{(L-2)}} \left(\dots W^{(1)} \cdot \Phi_{U^{(0)}} (m_{U^{(0)}}(A)) \dots \right) \right) \quad (16)$$

or recursively as follows

$$f^L(A) = W^{(L)} \cdot \Phi_{U^{(L-1)}} (f^{L-1}(A)) \quad (17)$$

where,

$$f^1(A) = W^{(1)} \cdot \Phi_{U^{(0)}} (m_{U^{(0)}}(A)) \quad (18)$$

here, “.” denotes matrix multiplication. To maintain submodularity, all weight matrices must be non-negative. A DSF can incorporate skip connections, and in general, a directed acyclic graph topology can be used to represent the DSF architecture with the help of recursive definitions (refer to section 4.1 of Bilmes and Bai [2017]).

Lastly, Bilmes and Bai [2017] showed that DSFs strictly generalize feature-based functions, and adding additional layers strictly increases the representation capacity, therefore suggesting the utility of additional layers!

D Weighted Matroid Rank Aggregation for DSFs

Vanilla DSFs use modular functions (sum operator) for permutation invariant aggregation. However, as we show in appendix B and definition 5, given a matroid $\mathcal{M} = (V, \mathcal{I})$ a modular function is indeed just a special case of a weighted matroid rank function. Moreover, another common permutation invariant aggregation technique - max-pooling is yet another special case of the weighted matroid rank function. Therefore, with the same notations as in appendix C we define a DSF via a weighted matroid rank as follows:

$$f_{\mathcal{M}}(A) = W^{(L)} \cdot \Phi_{U^{(L-1)}} \left(W^{(L-1)} \cdot \Phi_{U^{(L-2)}} \left(\dots W^{(1)} \cdot \Phi_{U^{(0)}} (\vec{\max}_{I \in \mathcal{I}} m_{U^{(0)}}(A \cap I)) \dots \right) \right) \quad (19)$$

where define $\vec{\max}$ as applying maximum operator to every index as follows:

$$\vec{\max}_{I \in \mathcal{I}} m_{U^{(0)}}(A \cap I) = \left(\max_{I \in \mathcal{I}} m_u(A \cap I) \mid u \in U^{(0)} \right)^T \quad (20)$$

In theorem 12 we show that $f_{\mathcal{M}}$ is a permutation invariant submodular set function. To show that $f_{\mathcal{M}}$ is submodular we first state some properties that will be useful. We re-visit the definitions from Bilmes and Bai [2017] for *superdifferential* and *antitone superdifferential* of a concave function which we will use to provide sufficient conditions that will help to show f is submodular.

Definition 8 (*Superdifferential*). *Let $\phi : \mathbb{R}^d \rightarrow \mathbb{R}$ be a concave function; a superdifferential of a concave function is a set defined as follows*

$$\partial\phi(x) = \{s \in \mathbb{R}^n : f(y) - f(x) \leq \langle s, y - x \rangle, \forall y \in \mathbb{R}^n\}$$

Definition 9 (*Antitone Superdifferential*). *A concave function $\phi : \mathbb{R}^d \rightarrow \mathbb{R}$ is said to have antitone superdifferential if for every $x \leq y$ (where ordering is defined for each dimension) we have a superdifferential $h_x \geq h_y$ for all $h_x \in \partial\phi(x)$ and for all $h_y \in \partial\phi(y)$.*

Using the definitions above, we have the following -

Lemma 10. *Given for every layer ℓ in a DSF the list of monotone non-decreasing normalized concave functions $\Phi_{U^\ell} = (\phi_u \mid u \in U^\ell)$, W be matrix of non-negative mixture weights. Define $\psi : \mathbb{R}^k \rightarrow \mathbb{R}$ as follows*

$$\psi(x) \triangleq W^{(L)} \cdot \Phi_{U^{(L-1)}} \left(W^{(L-1)} \cdot \Phi_{U^{(L-2)}} \left(\dots W^{(1)} \cdot \Phi_{U^{(0)}}(\vec{x}) \dots \right) \right) \quad (21)$$

Then ψ is concave and has antitone superdifferential.

Proof. The proof can be done following the similar steps as in Lemma 5.13, Corollary 5.13.1 and Lemma 5.14 from Bilmes and Bai [2017]. \square

We now re-state Theorem 5.12 in Bilmes and Bai [2017] as the follows.

Lemma 11. *Let $\psi : \mathbb{R}^k \rightarrow \mathbb{R}$ be a monotone non-decreasing concave function and let $\vec{g}(A) \triangleq (g_1(A), g_2(A) \dots g_k(A))$ be a vector of monotone non-decreasing and normalized submodular (polymatroid) functions. Then if ψ has an antitone super differential, then the set function $f : 2^V \rightarrow \mathbb{R}$ defined as $f(A) \triangleq \psi(\vec{g}(A))$ is submodular for every $A \subseteq V$.*

Proof. The proof is the same as for Theorem 5.12 in Bilmes and Bai [2017]. \square

Using the theorem above, we have the following corollary that shows the submodularity of the Deep Submodular Function defined using the weighted matroid rank ($f_{\mathcal{M}}(A)$) as the aggregation function.

Theorem 12 (*Submodularity of $f_{\mathcal{M}}$*). *Given a matroid $\mathcal{M} = (V, \mathcal{I})$, $\vec{g}(A) \triangleq (\max_{I \in \mathcal{I}} m_u(A \cap I) \mid u \in U^{(0)})^T$ and ψ as in lemma 10, $f_{\mathcal{M}}(A) = \psi(\vec{g}(A))$ is submodular $\forall A \subseteq V$. Moreover, $f_{\mathcal{M}}(A)$ is permutation invariant on the elements of set A .*

Proof. This is an application of lemma 10 into lemma 11 using the knowledge that weighed matroid rank are polymatroid functions. Permutation invariance of $f_{\mathcal{M}}$ it can be inferred from the permutation invariance of weighted matroid rank function from lemma 1 \square

This leads us to the fact that any DSPN, assuming that $w = (w_p, w_r)$ are valid (specifically, that $w_r \geq 0$) is submodular.

Theorem 2 (*A DSPN is monotone non-decreasing submodular*). *Any DSPN $f_w(A) = \psi_{w_r}(h_{w_p}(A))$ so defined is guaranteed to be monotone non-decreasing submodular for all valid values of w .*

Proof. The output of each pillar is a d -dimensional non-negative vector. The aggregation via any weighted matroid rank of the pillar outputs for any set $A \subseteq V$ is also a d -dimensional non-negative vector and moreover, each element of this resulting aggregated vector is itself a polymatroid function thanks to the fact that a weighted matroid rank function is a polymatroid function. When we compose a vector of polymatroid functions with a DSF, this preserves polymatroidality by Theorem 5.12 in Bilmes and Bai [2017], and thus submodularity. The theorem is hence proven. \square

Corollary 3 (*Submodular Preservation of Weighted Matroid Rank Aggregators*). *Any weighted matroid rank function for matroid $\mathcal{M} = (V, \mathcal{I})$ with any non-negative vector $m \in \mathbb{R}_+^{|V|}$, when used as an aggregator in a DSPN, will be submodularity preserving.*

Proof. This follows immediately from Theorem 2. \square

E Further discussion on (E,M) pair sampling and dataset construction strategies

Training a DSPN via the peripetal loss requires transferring information from an expensive oracle target function to a learnt DSPN. As mentioned in §section 4, this requires a dataset $\mathcal{D} = \{(E_i, M_i)\}_{i=1}^N$ of pairs of sets to be contrasted with each other where each $E_i, M_i \subseteq V$. The target function in our work is an expensive facility location function, but in general it can be any oracle to provide information in a GPC context to a learner. This means that $\Delta(E|M) = f_t(E) - f_t(M)$. As submodular functions are set functions that tend to produce higher score for a diverse set and a low score for a homogeneous set, the oracle evaluation will be positive if E is considered more diverse than M and will be negative if M is considered more diverse than E . For this reason, even if we design sampling strategies that attempt to produce pairs E, M where E is more diverse than M , the peripetal loss Eqn. (3) allows for mistakes to be made in the selection of these pairs since the sign of the oracle GPC can switch within the peripheral loss. Hence, our approach is robust to E, M pair label noise in this sense. This also means that our E, M sampling strategy can be done in an automated manner.

Moreover, a set E might be seen as diverse in some cases and homogeneous in other cases. For instance, a set E containing elements from two distinct classes is heterogeneous compared to a set M containing all elements from one class. However, the same set E is homogeneous when compared against a set E' containing all distinct classes, so in this latter case the (E, M) pair would be (E', E) . The oracle query offers a GPC of the pair (E, M) providing a score $Score(A, B) \in \mathbb{R}$ depending on which of E and M is more diverse. The pairwise comparison aspect of GPC is one of its powers since we are not asking for absolute scores from the oracle but for comparisons between pairs. This is one of the benefits of pairwise comparison models when querying humans as well (as discussed in the field of psychometrics Nunnally and Bernstein [1994] and this benefit extends to the GPC case as well Lingel et al. [2022]).

For learning a DSPN, an oracle evaluation will require evaluations with an expensive FL function, but in general the oracle need not be submodular at all, and can even be a non-submodular arbitrary dispersion function. Furthermore, as mentioned above, our framework only requires query access to the oracle, we do not need to optimize over it. When the target is non-submodular and we are learning a DSPN, our approach can be seen as finding a projection of a non-submodular function onto the space of DSPNs. A compelling example of this is in the context of dataset pruning, where a target function could be a mapping from pairs of subsets of training data to the difference in validation accuracies that a deep model achieves after being trained on each of the subsets and evaluated on a validation set (we do not test this case in this paper however, but plan to do so in future work). An alternate target function could capture a human’s assessment of diversity of a summary, incorporating human feedback into the process of learning a submodular function. Crucially, in both of these examples, the target functions are not directly optimized but are only queried. Our framework may allow us to distill them onto easy-to-optimize functions such as DSPNs that can still exhibit essential and relevant properties of the target.

In general, how the (E, M) pair of subsets are chosen in the learning procedure is absolutely critical, and this is why we have introduced a suite of novel automatic sampling strategies. One of the strategies involves passive sampling of sets via random subsetting and clustering. The other strategy is a new “submodular feedback” method that can be seen as combinatorial active learning since it optimizes over the DSPN as it is being learnt to produce the (E, M) sets, something greatly facilitates learning.

F Analysis of Peripetal Loss

In addition to the motivation for our loss function provided in section 3 here we provide a discussion on its gradient and curvature and how the hyperparameters govern the curvature of the provided loss. First, we re-state the *mother* loss, plot its value for different values of margin, and then follow by equation for its gradient and double-derivative. In the below $\sigma(x)$ refers to sigmoid function, that is, $\sigma(x) = \frac{1}{1+e^{-x}}$ and $\text{sgn}(x)$ refers to the sign of x .

The mother loss has the form

$$\mathcal{L}_\Delta(\delta) = |\Delta| \log(1 + \exp(1 - \frac{\delta}{\Delta})), \quad (22)$$

and the corresponding gradient becomes

$$\frac{\partial \mathcal{L}_\Delta(\delta)}{\partial \delta} = -\text{sgn}(\Delta) \sigma\left(1 - \frac{\delta}{\Delta}\right). \quad (23)$$

We first plot the loss and the gradients in fig. 7. From the plots in fig. 7 and gradient in eq. (23), it is clear that if Δ is (very) positive, then δ must also be (very) positive to produce a small loss. If Δ is (very) negative then so also must δ be to produce a small loss. The absolute value of Δ determines how non-smooth loss is so we include an outer pre-multiplication by $|\Delta|$ ensures gradient of loss, as a function of δ , asymptotes to negative one (or one when Δ is negative) in the penalty region, analogous to hinge loss, and thus produces numerically stable gradients.

Having established the ‘‘mother’’ loss $\mathcal{L}_\Delta(\delta)$ we can see that Δ controls its curvature (the smaller the $|\Delta|$ the higher the curvature). However, for each example, this margin would be different, and therefore, to provide global control over the curvature of the loss, we smooth it out using β in a way that produces smoother, more stable, and convergent optimization. This leads to the following loss (in addition to the explanation provided in the section 3)-

$$L_{\Delta; \beta, \tau, \kappa, \varepsilon}(\delta) = \frac{|\kappa\Delta + \varepsilon \text{sgn} \Delta|}{\beta} \log(1 + \exp(\beta(\tau - \frac{\delta}{\kappa\Delta + \varepsilon \text{sgn} \Delta}))) \quad (24)$$

and the corresponding gradient will be -

$$\frac{\partial L_{\Delta; \beta, \tau, \kappa, \varepsilon}(\delta)}{\partial \delta} = -\text{sgn}(\Delta) \sigma\left(\beta\left(\tau - \frac{\delta}{\kappa\Delta + \varepsilon \text{sgn} \Delta}\right)\right) \quad (25)$$

We plot the gradients in appendix F for two offsets, namely $\tau = 1$ and $\tau = 5$. From these plots, it is clear that β provides control over the smoothness of $L_{\Delta; \beta, \tau, \kappa, \varepsilon}(\delta)$ where the smaller the β the smaller the curvature (without impacting the gradient magnitudes). The importance of low curvature of the loss objective has been studied from the optimization stability Gilmer et al. [2021] as well as from the lens of robustness in deep learning Srinivas et al. [2022], Foret et al. [2021]. Similarly, we can also see that τ merely provides an offset in the gradient, which, however, can nevertheless be important for the gradient magnitude while we are optimizing.

Lastly, to account for corner cases where Δ is very small,

$$L_{\Delta; \alpha, \beta, \tau, \kappa, \varepsilon}(\delta) = \tanh\left(\frac{\alpha}{|\kappa\Delta|}\right) |\delta| + (1 - \tanh\left(\frac{\alpha}{|\kappa\Delta|}\right)) \mathcal{L}_{\Delta; \beta, \tau, \kappa, \varepsilon}(\delta) \quad (26)$$

and the corresponding gradient will be -

$$\frac{\partial L_{\Delta; \alpha, \beta, \tau, \kappa, \varepsilon}(\delta)}{\partial \delta} = \tanh\left(\frac{\alpha}{|\kappa\Delta|}\right) \text{sgn}(\delta) + (1 - \tanh\left(\frac{\alpha}{|\kappa\Delta|}\right)) \frac{\partial \mathcal{L}_{\Delta; \beta, \tau, \kappa, \varepsilon}(\delta)}{\partial \delta} \quad (27)$$

Note that for $\delta = 0$ the function is indeed non-differentiable, however, we can have any subgradient between $[-1, 1]$. Similar to PyTorch Paszke et al. [2019] we choose to have the subgradient to be 0, as $|\delta|$ is also 0 at that point. In practice, we do not encounter any instabilities due to this, and gate value throughout our experiments remains very small.

G Periperial Networks and Training Flow

Figure 11 depicts the DSPN architecture. In fact, we see two copies of a DSPN presented in Figure 11, the left one instantiated for the E set and the right one instantiated for the M set. Each DSPN consists of a set of pillars which transform a number of objects (e.g., images corresponding to a set) into a

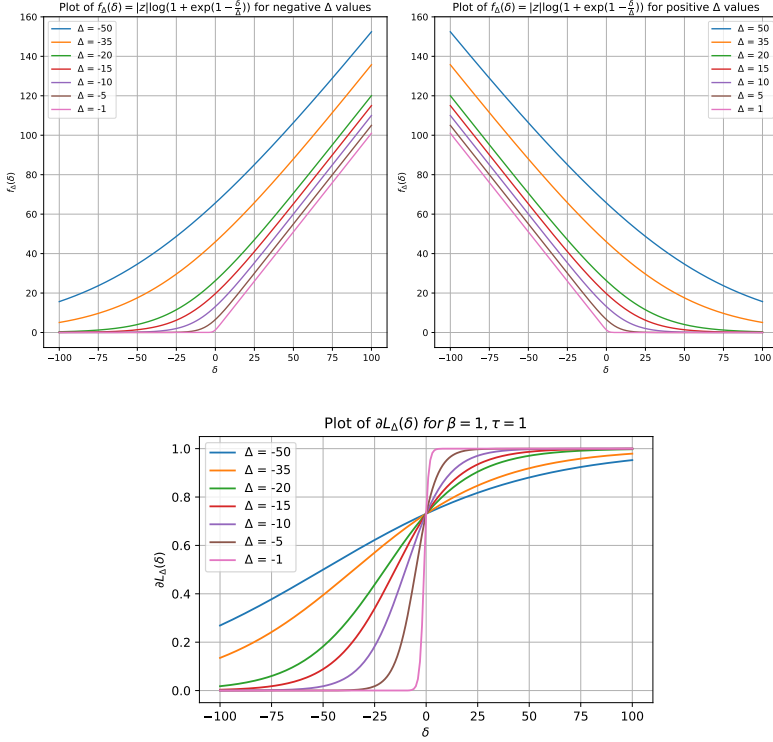


Figure 7: Peripetal loss of δ for different values and sign of margin Δ and the corresponding gradient.

non-negative embedding space. The reason for the space to be non-negative is to ensure that the subsequent transformations can preserve submodularity, in the same way that a concave composed with a modular function requires the modular function to be non-negative to preserve submodularity. The figure above shows that object space has dimension nine (the number of red nodes on the bottom of each pillar) and embedding space having dimension seven (the seven orange nodes at the top of each pillar). This DSPN has five pillars which means that it is appropriate for an E or M set of size five. The outputs of the pillars are aggregated using a submodular-preserving permutation invariant aggregator (such as a weighted matroid rank function) but in the experiments in this paper, we use a simple uniform matroid which corresponds to a summation aggregator. Note that each scalar output of each pillar is aggregated separately and after aggregation we get a resulting seven-dimensional vector which is input to a deep submodular function (DSF). We consider the aggregation step and the final DSF to be the ‘‘roof model.’’, highlighted with the blue triangle above. The word **peripetal** is an adjective (applicable typically to a building) which means having a single row of pillars on all sides in the style of the temples of ancient Greece. This is reminiscent of the above DSPN structures which is the reason for this name.

To train a DSPN, we need two sets, an E (hEterogeneous) set and an M (hOMogeneous) set. Each of the E and M sets of the (E, M) pair is presented to a DSPN instantiation being learnt and which is governed, overall by the parameters w . Note that w consists both of the parameters for the DSPN pillars as well as the parameters for the DSPN roof. The parameters for all instances of the pillar are shared over all pillars, similar to how Siamese networks share (or tied) parameters between the two transformations. Here, however the number of pillars in the DSPN grows or shrinks depending on the sizes $|E|$ and $|M|$ of the sets E and M respectively, but regardless of the size of $|E|$ or $|M|$ the number of the parameters of the pillars stays fixed. These sets are acquired in a variety of different ways, and this includes heuristics on the data (e.g., clusterings, random sets) as well as submodular feedback strategy which optimizes the DSPN as it is being learnt to ensure that what the DSPN thinks has high or low value agrees with the target oracle.

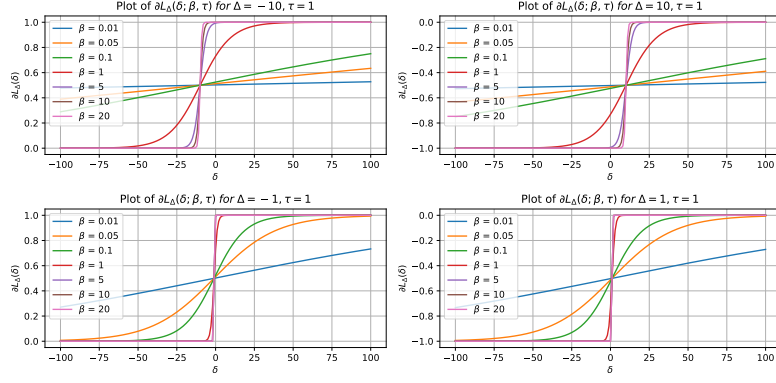


Figure 8: $\tau = 1$.

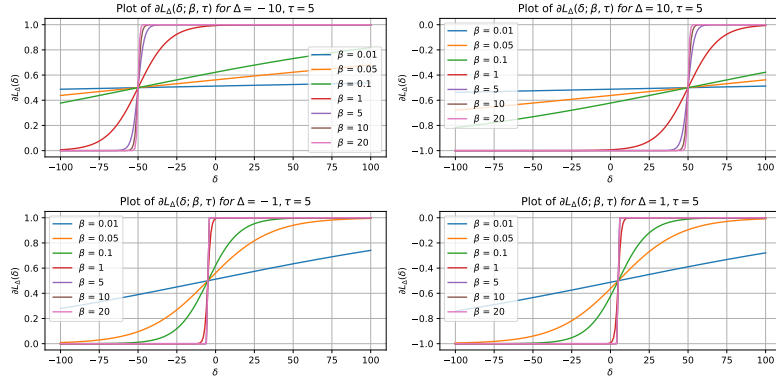


Figure 9: $\tau = 5$

H Additional Experimental Details

Baseline Loss Functions To assess the efficacy of our peripetal loss, we consider two popular baselines to learn from pairwise comparisons. Note that we only replace our peripetal loss function with the baseline and we do not remove any necessary regularizers such as \mathcal{L}_{redn} and \mathcal{L}_{aug} . Using the same notations as the main paper, we define the regression loss \mathcal{L}_{regr} and \mathcal{L}_{marg} in equations 28 and 29.

$$\mathcal{L}_{regr}(f_w; \Delta(E|M), \delta_{f_w}(E|M)) = (\delta_{f_w}(E|M) - \Delta(E|M))^2 \quad (28)$$

$$\mathcal{L}_{marg}(f_w; \Delta(E|M), \delta_{f_w}(E|M)) = \max(\Delta(E|M) - \delta_{f_w}(E|M), 0) \quad (29)$$

Given the dataset $\mathcal{D} = \{(E_i, M_i)\}_{i=1}^N$ of pairs, we have the following empirical risks for regression (Eq. 30) and margin (Eq. 31).

$$\begin{aligned} \hat{\mathcal{R}}_{regr}(w; \mathcal{D}) = & \frac{1}{N} \sum_{i \in [N]} (\mathcal{L}_{regr}(f_w; \Delta(E_i|M_i), \delta_{f_w}(E_i|M_i)) + \mathcal{L}_{aug}(f_w; E \cup M, E' \cup M') \\ & + \mathcal{L}_{redn}(f_w; E, E') + \mathcal{L}_{redn}(f_w; M, M')) \end{aligned} \quad (30)$$

$$\begin{aligned} \hat{\mathcal{R}}_{marg}(w; \mathcal{D}) = & \frac{1}{N} \sum_{i \in [N]} \mathcal{L}_{marg}(f_w; \Delta(E|M), \delta_{f_w}(E|M)) + \mathcal{L}_{aug}(f_w; E \cup M, E' \cup M') \\ & + \mathcal{L}_{redn}(f_w; E, E') + \mathcal{L}_{redn}(f_w; M, M')) \end{aligned} \quad (31)$$

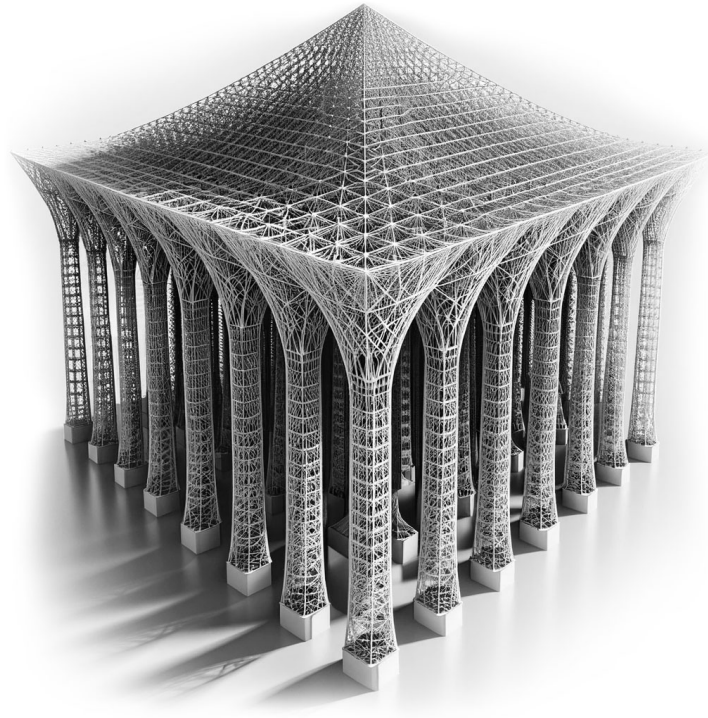


Figure 10: A “peripteral neural temple” showing a Greek/Roman style peripteral structure with many pillars rendered as a form of neural temple, where each of the pillars, the submodular preserving and permutation-invariant aggregation, and the roof are all seen as having an underlying neural network graphical structure.

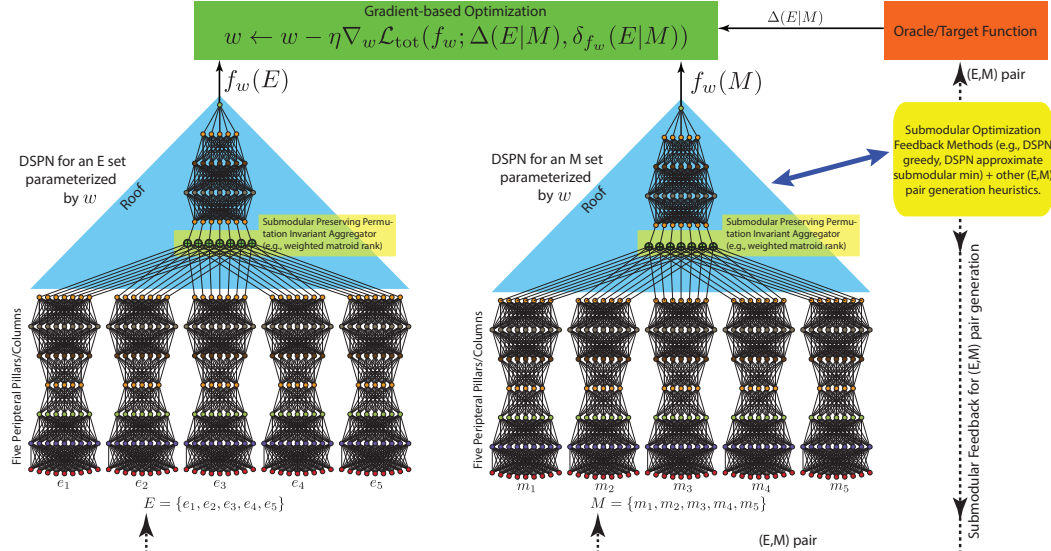


Figure 11: The figure shows the structure of a DSPN as well as the control flow of how a DSPN is trained.

Hyperparameters We train every DSPN on 2 NVIDIA-A100 GPUs with a cyclic learning rate scheduler Smith [2017], using Adam optimizer Kingma and Ba [2014]. To ensure non-negative parameters in DSF, we perform projected gradient descent, where we apply projection on ψ_{w_r} to the non-negative orthant after every gradient descent step.

We list the hyperparameters we use for the periperial loss in table 2 and table 3. We observed that β and τ are the most salient hyperparameters since they control the curvature and hinge of the loss respectively. The benefits of smaller loss curvature have been widely studied from optimization stability in deep learning Gilmer et al. [2021], Srinivas et al. [2022], Foret et al. [2021] and our low value of β corroborates with the previous works. α parameter controls the tanh gate, the smaller the value of alpha the more weightage of our objective function. Since we did not encounter corner cases where Δ is very small, neither ϵ nor α were found to be salient.

	α	β	κ	τ	ϵ
Imagenette	$1e - 5$	0.5	1	10	$1e - 15$
Imagewoof	$1e - 5$	0.5	1	10	$1e - 15$
CIFAR100	$1e - 5$	0.01	1	10	$1e - 15$
Imagenet100	$1e - 5$	0.01	1	10	$1e - 15$

Table 2: Periperial loss hyperparameters used for each dataset. λ_1 and λ_2 correspond to the coefficients used in the augmentation regularizer (Eq. 4, while λ_3 and λ_4 are the coefficents in (Eq. 5)

	λ_1	λ_2	λ_3	λ_4
Imagenette	0.25	0.01	0	0
Imagewoof	0.25	0.01	0	0
CIFAR100	0.25	0.01	$1e - 5$	$5e - 4$
Imagenet100	0.25	0.01	0	0

Table 3: Loss coefficients used for each dataset.

Dataset Construction We compute the passive (E, M) pairs offline to improve computational efficiency. For the actively sampled pairs, we generate (E, M) pairs every K epochs where an epoch is defined as a full pass over all of the offline pairs. For all the datasets we consider, $K = 15$.

Long-tailed Dataset Construction For the results presented in Sections 5.2, we create pathologically imbalanced datasets from sets of images that the DSPN never encountered during training. Specifically, we add duplicates for each image in a class; the number of duplicates varies per class and is drawn from a Zipf distribution Zipf [2013]. We show the final distributions of the imbalanced dataset in Figure 12.

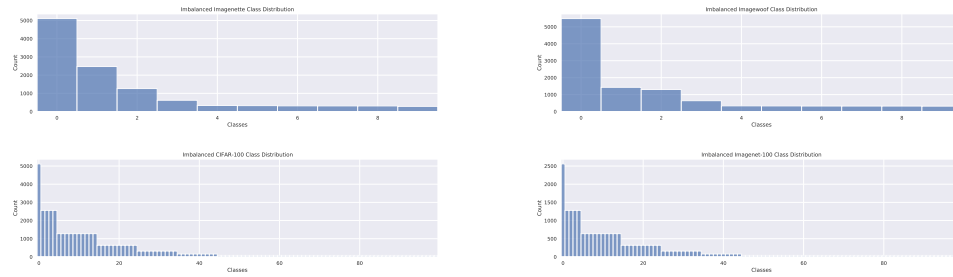


Figure 12: Imbalanced dataset distributions

I Qualitative Analysis of Learnt Features

In Table 1, we show that imparting DSPNs the ability to learn features is crucial for successful training. Feature-based functions and DSFs work best when features correspond to some bag-of-words or

count like attribute. For example, Lin and Bilmes [2012], Liu et al. [2013] both use TF-IDF based feature extractors to instantiate feature-based functions. More recently, Lavania and Bilmes [2019] learns “additively contributive” (AC) features with an autoencoder by restricting all weights in the initial layer of the decoder to the positive orthant. Unfortunately, universal features for images procured from modern pretrained models such as CLIP do not necessarily have this property.

We show that DSPNs learn bag-of-words features in Figure 13, by exploring the preferences of individual DSPN/CLIP features. For visualization purposes, we randomly select 10 features from the model in consideration and use each feature to rank the images from a held out set. The top 10 images selected by any of the DSPN features appear very homogeneous and are strongly correlated to class, while images with the lowest feature values (typically with feature value 0) are practically indistinguishable from a random subset of images. In other words, a high value indicates the *presence* of some attribute while a low value indicates its *absence*. When we perform a similar qualitative analysis upon CLIP features, we find that both the high valued sets and low valued sets have some weak correlation to class. CLIP features cannot be interpreted in the same way as DSPN because each feature corresponds to a coordinate in some higher dimensional space. Our results show that features that encapsulate count-like attributes are essential for learning a good DSF.



Figure 13: Qualitative Assessment of Learnt Features on Imagenet100. For each row, we use a randomly selected feature of either DSPN or CLIP to rank all images in the held out set and visualize the highest and lowest ranked samples. Each DSPN feature corresponds to some count-like property that is correlated to class, evident from the fact that very few distinct classes are present in the highly ranked images.